SAND2018-10885C

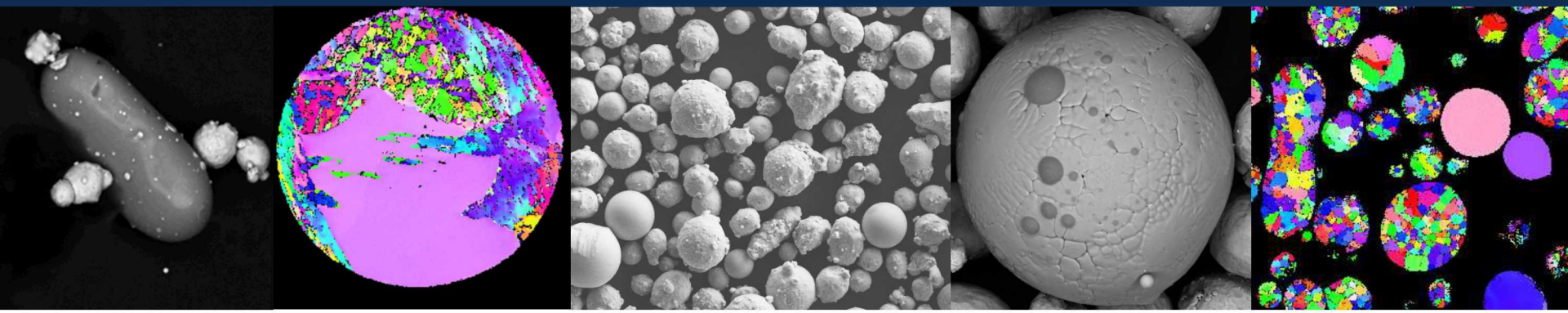

Metal Powder Feedstock Reuse in Additive Manufacturing: Characterization of 316L Stainless Steel

Michael Heiden, Jeff Rodelas, Lisa Deibler, Josh Koepke, Dan Tung, David Saiz, Bradley Jared

Sandia National Laboratories, Albuquerque, NM

Sandia National Laboratories is a multimission laboratory managed and operated by National Technology and Engineering Solutions of Sandia LLC, a wholly owned subsidiary of Honeywell International Inc. for the U.S. Department of Energy's National Nuclear Security Administration under contract DE-NA0003525.

Motivation for study on powder reuse

- Currently 5-46% of cost in PBF is feedstock; reuse reduces costs [1]
- 50-90% of the build area is unused powder [1]
- Still relatively unknown how heat-affected powders change and affect part properties
- Variability in mechanical properties may partially be due to quality of feedstock

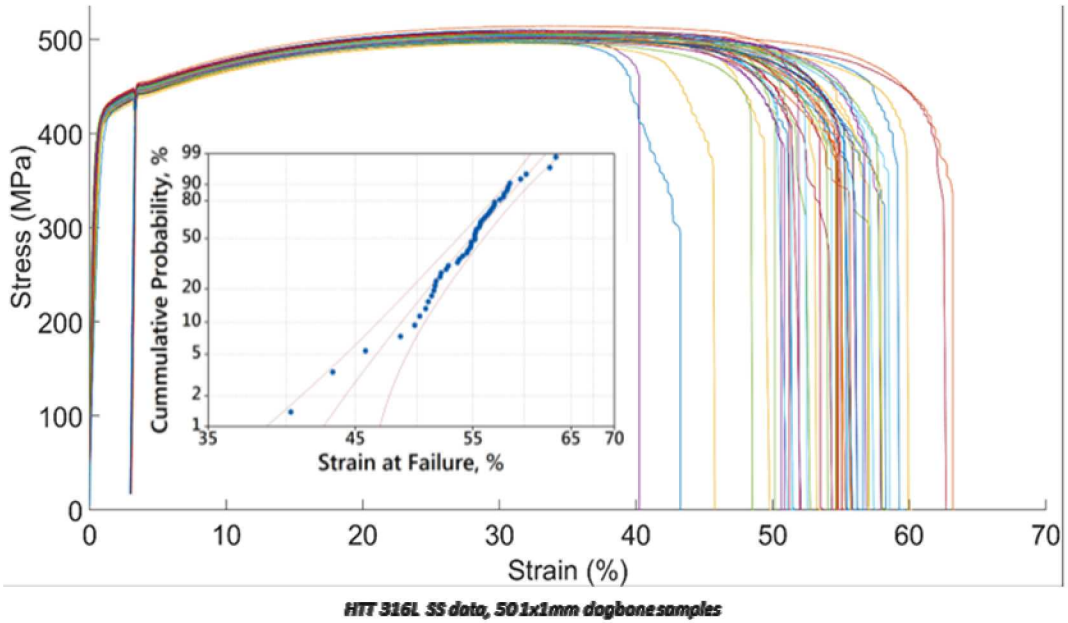

HIT 316L SS data, 501x1mm dogbone samples

To improve reusability/recyclability of powders, this study aims to determine:

- How does the energy source degrade feedstock quality?
- How do particle properties affect variability in final part properties?

1. Caitlin Kriewall, A. Sutton, S. Karnati, J. Newkirk, M. Leu, Effects of Area Fraction and Part Spacing on Degradation of 304L Stainless Steel Powder in Selective Laser Melting, Solid Freeform Conference, 2017.

Dynamic SLM laser-powder interactions

- Vaporization of alloy species
- Particle fusion near weld pool
- Particle collisions
- Melt pool ejecta/spatter
- Gas entrainment of nearby particles
- Denudation
- Satellite formation
- Clusters/agglomerates

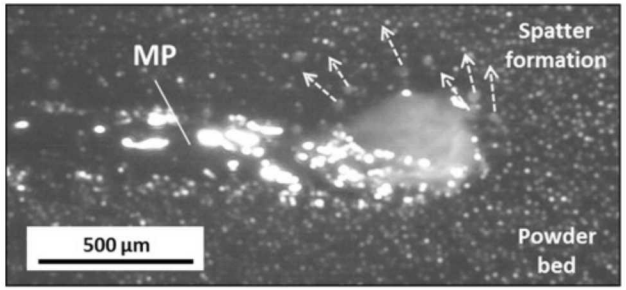

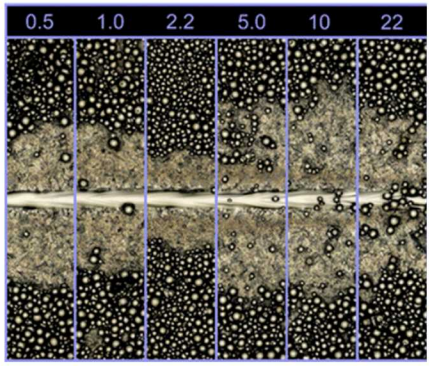

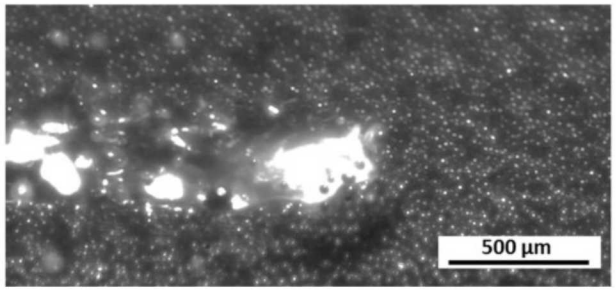

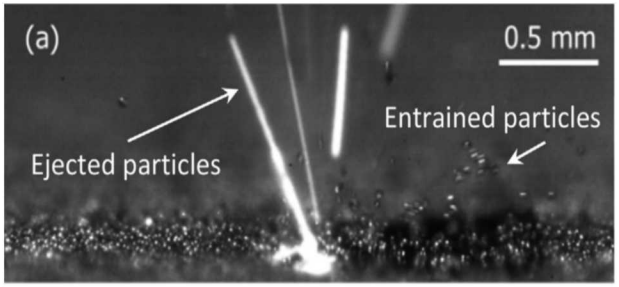

Need to understand powder reuse effects→ apply characterization techniques to understand attribute changes as a function of reuse

S. Ly, A.M. Rubenchik, S.A. Khairallah, G. Guss, M.J. Matthews, Sci Rep 7(1) (2017) 4085
V. Gunenthiram, P. Peyre, M. Schneider, M. Dal, F. Coste, R. Fabbro, Journal of Laser Applications 29(2) (2017)
P. Bidare, I. Bitharas, R. M. Ward, M. M. Attallah, A. J. Moore, Acta Materialia 142 (2018) 107-120
M.J. Matthews, G. Guss, S.A. Khairallah, A.M. Rubenchik, P.J. Depond, W.E. King, Acta Materialia 114 (2016) 33-42

Outline – 316L characterization

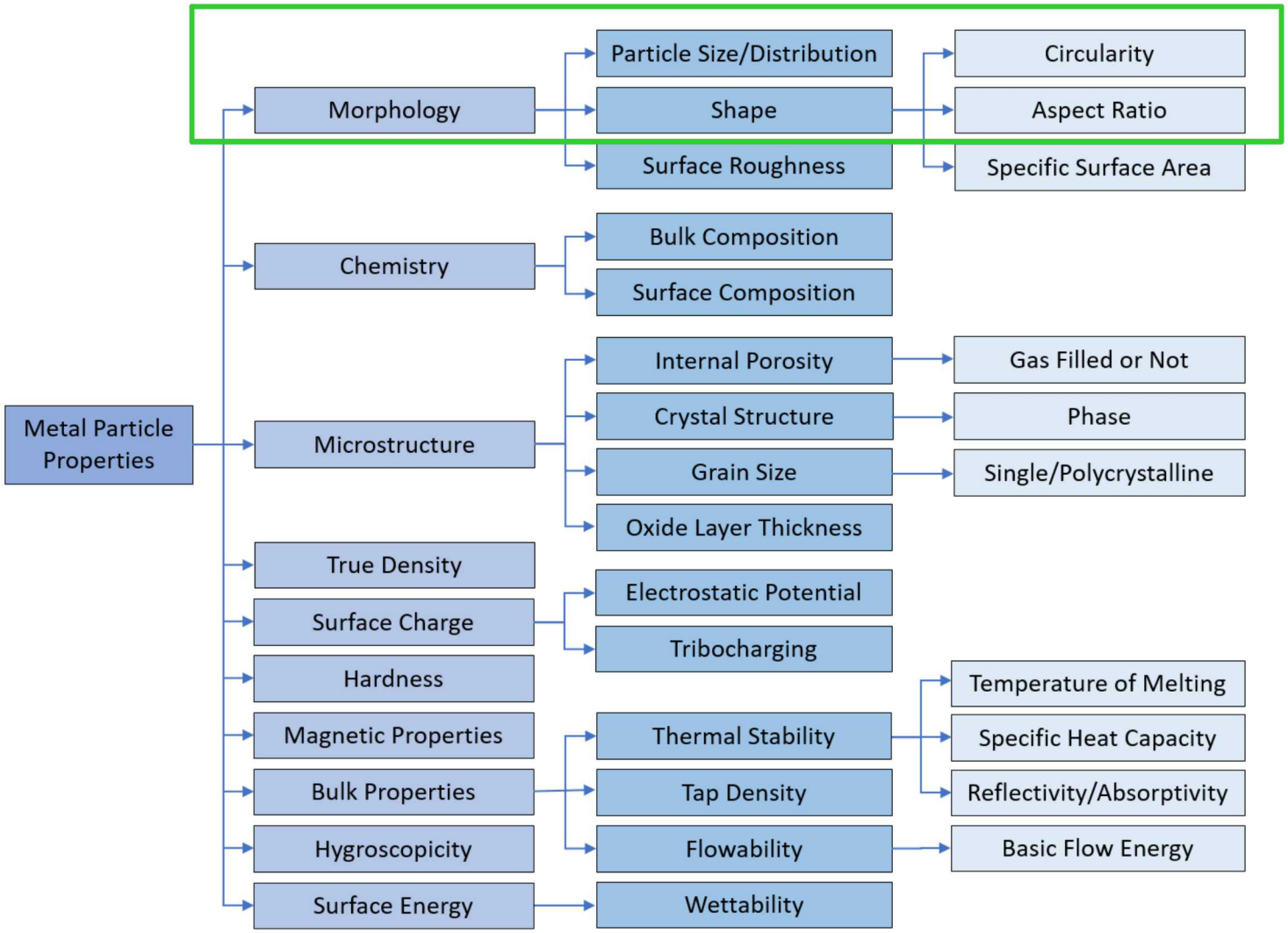

- Each powder batch was sieved between multiple build cycles, with a total ‘reuse’ of 30 times

No major change to PSD with 30 reuses

Sandia National Laboratories

Differential Size Distribution

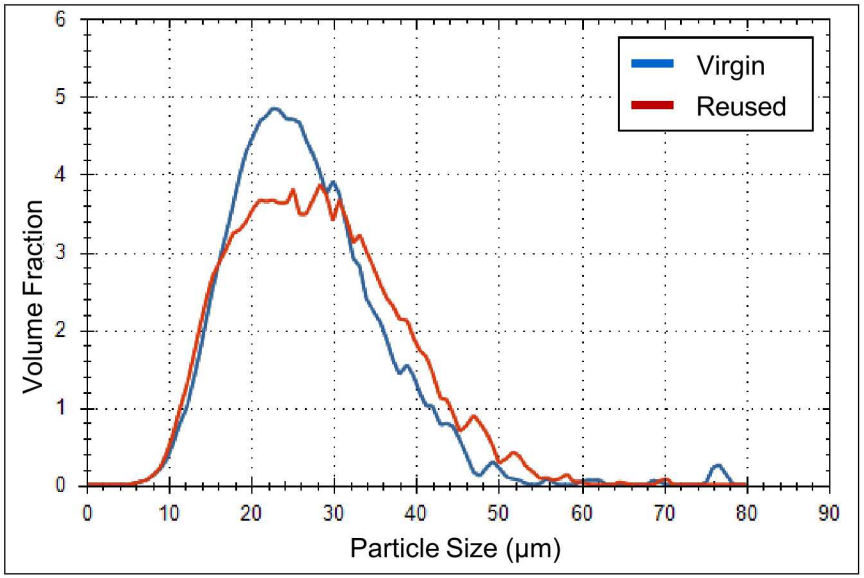

Cumulative Size Distribution

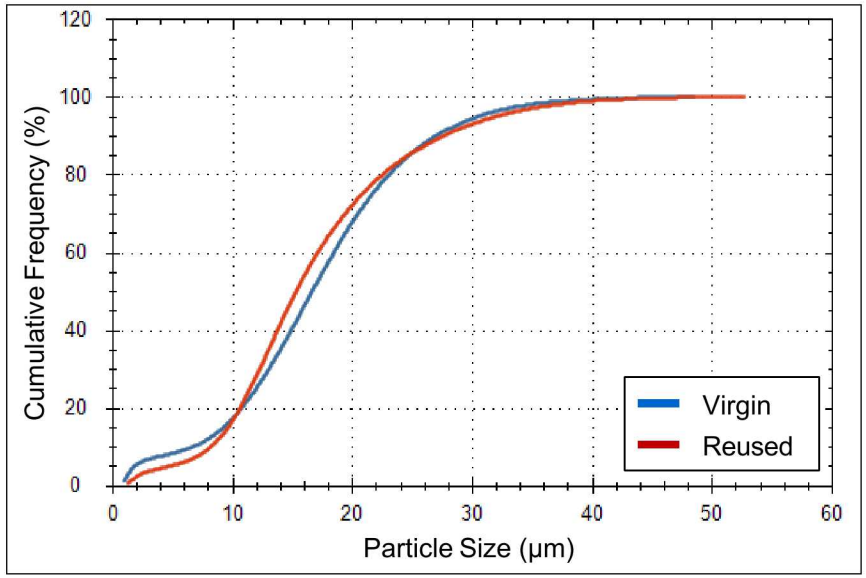

(based on cumulative number frequency)						
Powder (Stdev)	Average Dia. (µm)	D_n10 (µm)	D_n50 (µm)	D_n90 (µm)	Aspect Ratio	Circularity
Virgin	16.4 (1.7)	7.0 (3.3)	16.9 (2.9)	26.9 (2.2)	0.68 (0.04)	0.83 (0.07)
Reused	16.9 (1.2)	8.2 (1.3)	15.4 (1.0)	27.5 (2.2)	0.66 (0.05)	0.81 (0.08)
(based on volume fraction)						
Powder (Stdev)	Average Dia. (µm)	D_v10 (µm)	D_v50 (µm)	D_v90 (µm)		
Virgin	22.4 (0.2)	13.6 (0.1)	21.1 (0.2)	32.7 (0.4)	-	-
Reused	35.7 (3.1)	17.2 (1.1)	27.1 (0.5)	59.3 (16.9)	-	-

- Particle size distribution shifts right
- Reduction in fine particles (<10 µm)
- Slight increase in amount of larger particles
- Wider particle distribution (volume fraction) with reuse

Satellites, agglomeration, and smooth particles

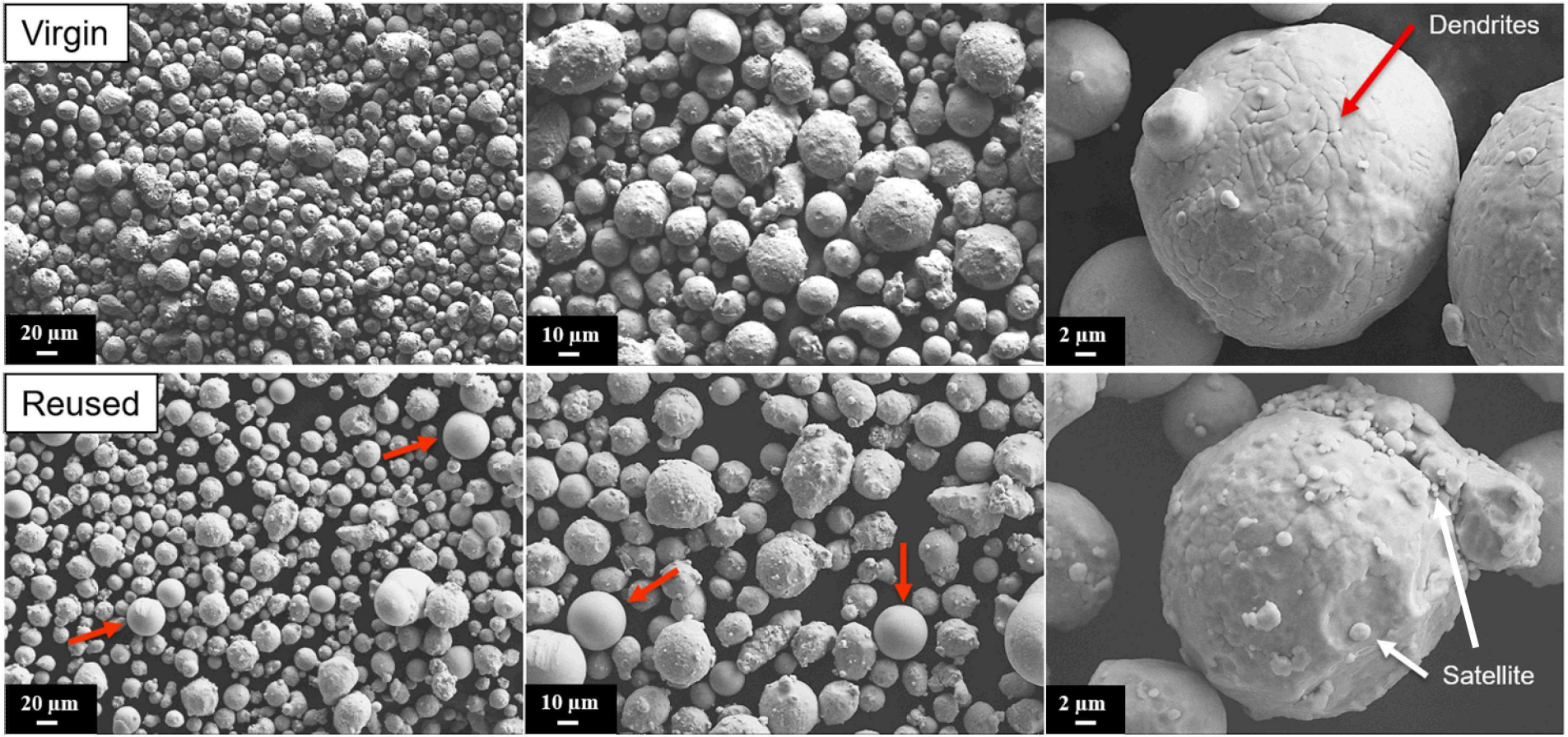

- Reused powder has significantly more satellite formation and agglomerates
- Reused contains substantial amount of highly spherical particles
- Can view solidification substructure on each virgin particle, not always for reused

Outline – Bulk composition analysis

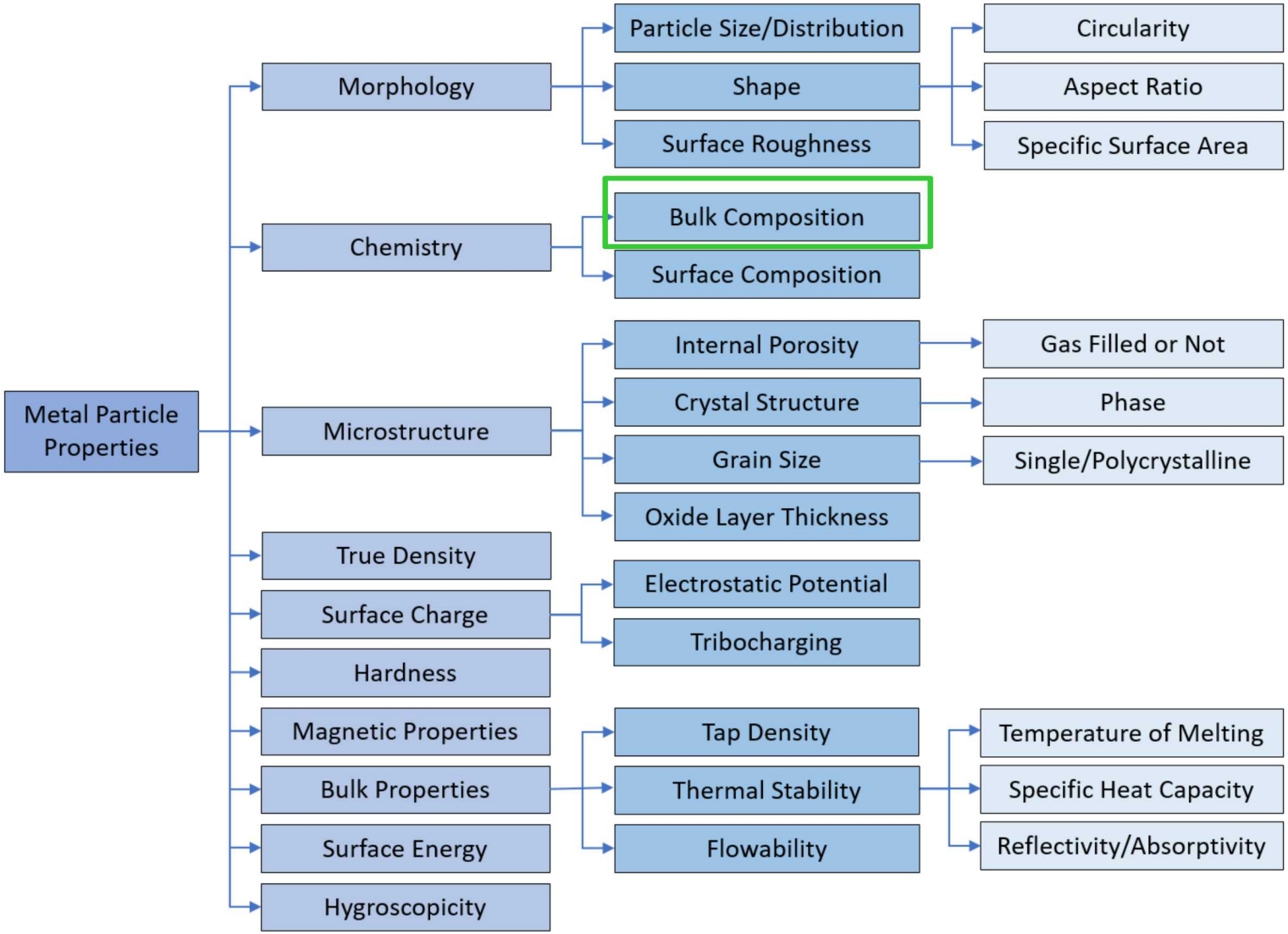

No major changes to powder bulk composition

Sandia National Laboratories

ICP-MS analysis

Wt.% (Stdev)	Fe	Cr	Ni	Mo	Si	Mn	Cu	P	Co	C	S	O	N
Virgin	67.8 (0.3)	16.84 (0.34)	10.81 (0.22)	2.05 (0.20)	0.65 (0.10)	1.20 (0.12)	0.21 (0.03)	0.015 (0.002)	0.098 (0.015)	0.011 (0.002)	0.014 (0.002)	0.067 (0.010)	0.086 (0.013)
Reused	67.6 (0.3)	16.91 (0.34)	10.90 (0.22)	2.02 (0.20)	0.60 (0.09)	1.27 (0.13)	0.22 (0.03)	0.016 (0.002)	0.11 (0.016)	0.016 (0.002)	0.014 (0.002)	0.095 (0.014)	0.090 (0.013)
ASTM Spec [2]	61-69	16-18	10-14	2-3	1 max	2 max	-	0.045 max	-	0.03 max	0.03 max	-	-

- O and C increased slightly with 30 reuses
- Differences for other elements within uncertainty range
- All compositions within ASTM spec

[2] ASTM F3184-16 Standard Specification for Additive Manufacturing Stainless Steel Alloy (UNS S31603) with Powder Bed Fusion, ASTM International ASM Handbook (2016) 1-9.

Outline – Microstructural changes

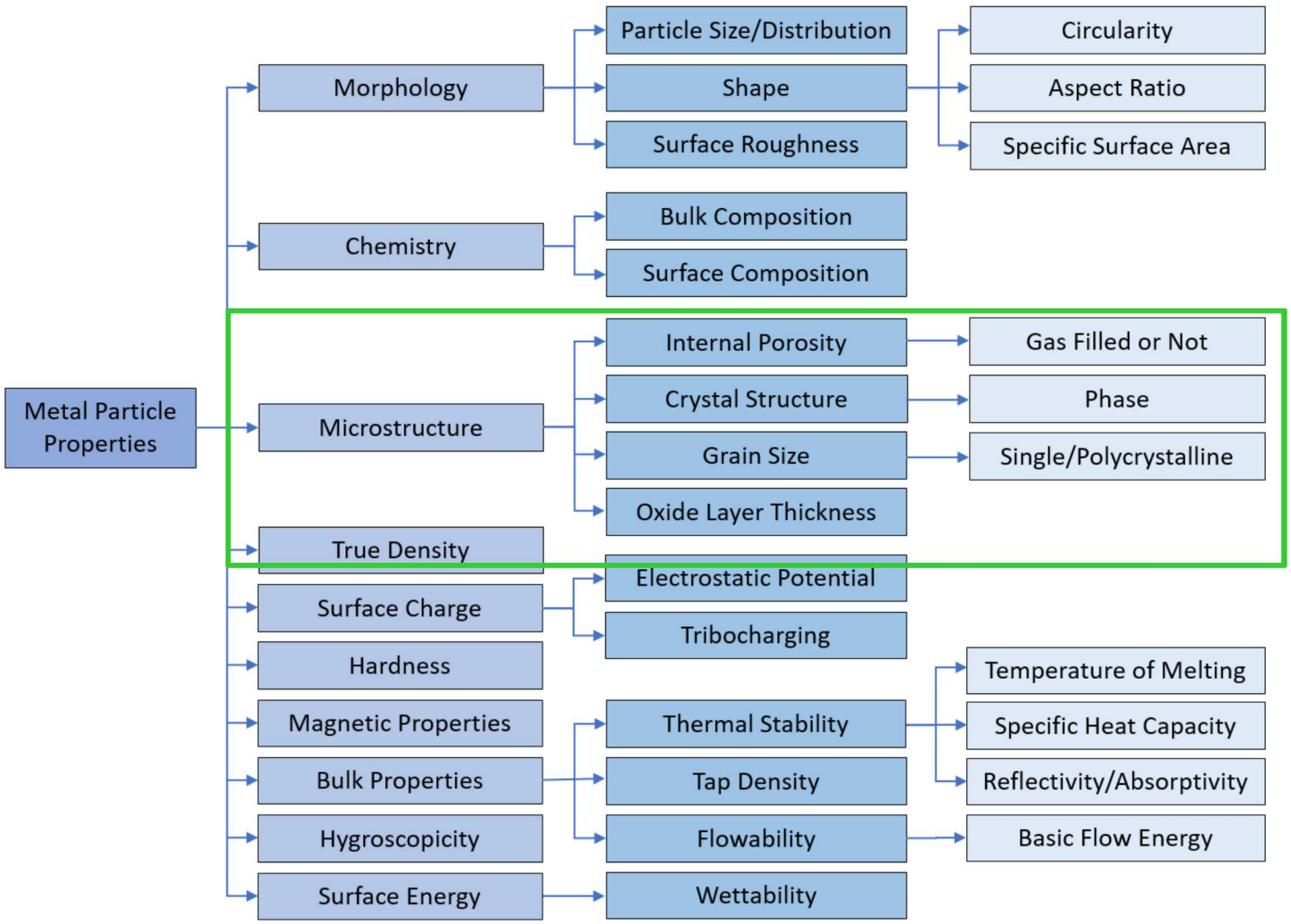

TEM shows increased oxide thickness with reuse

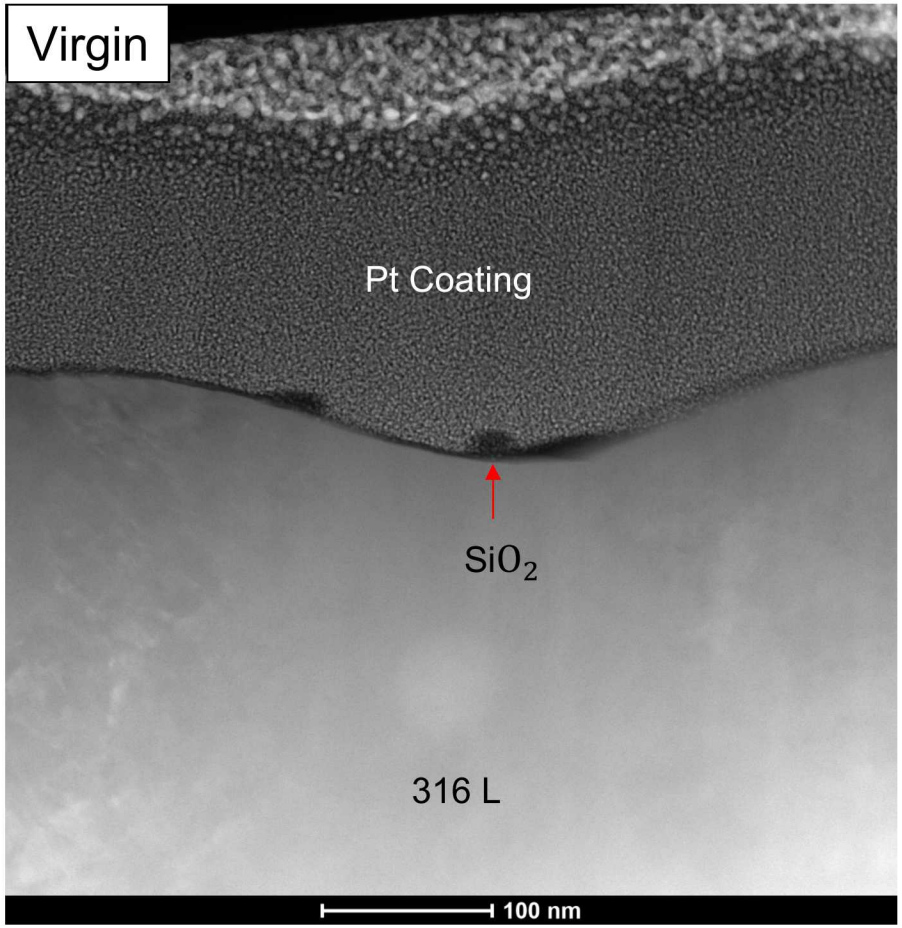

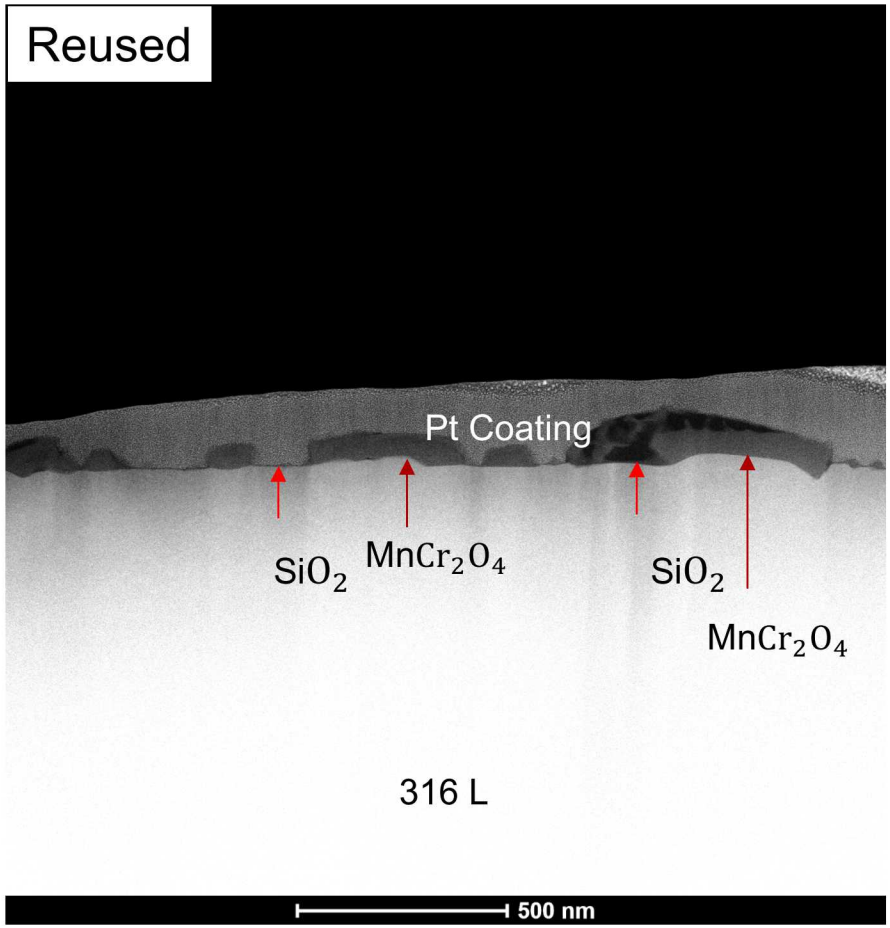

Oxide Layer	Virgin	Virgin Nodules	Reused	Reused Nodules
Average (nm)	3.7	14.8	4.4	79.5
Stdev (nm)	0.5	2.6	1.1	30.1

- Reuse generates oxide nodules across particle surface, which eventually grows into full layer

Varying levels of porosity in all powder samples

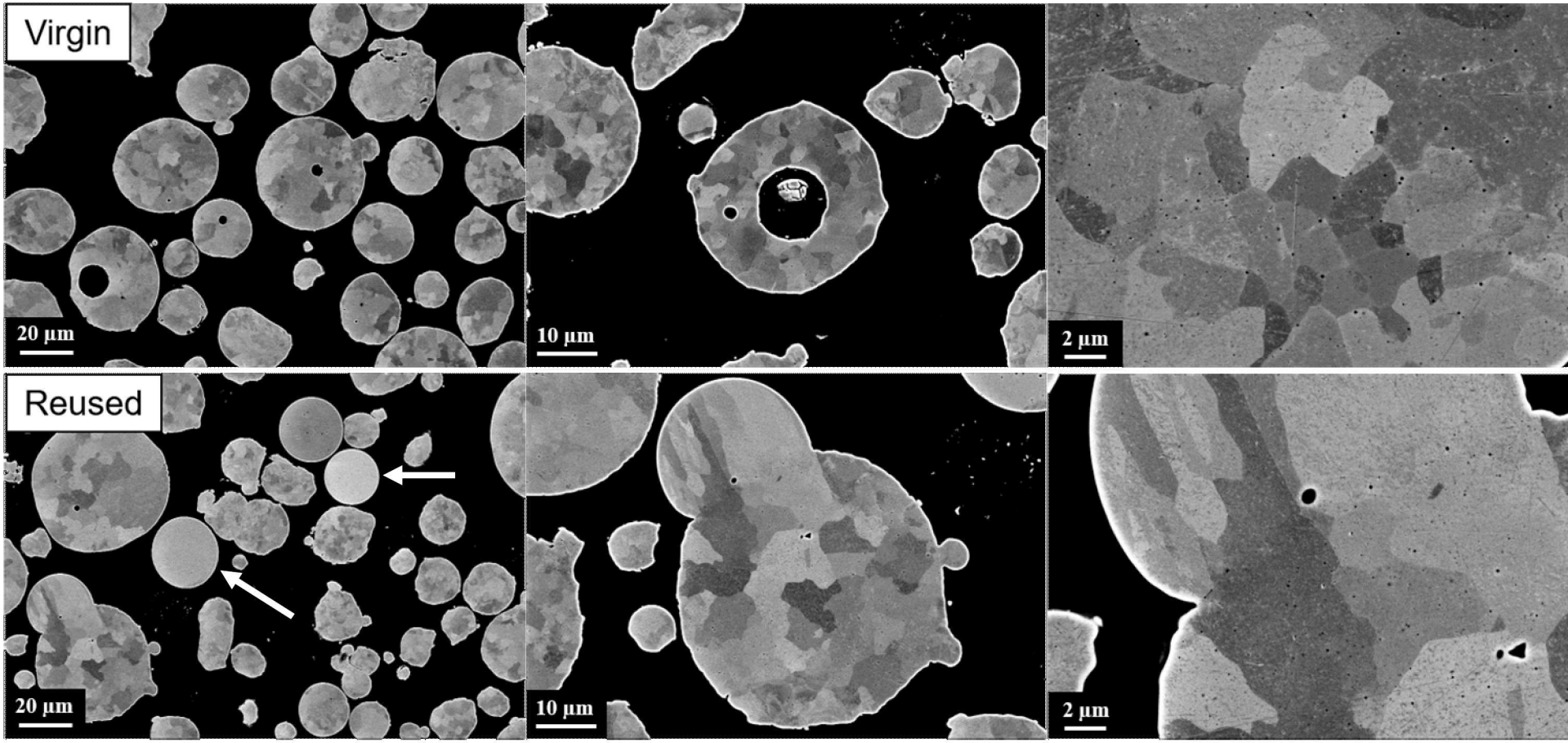

- Some reused particles contained no grain boundaries
- Slight reduction in true particle density

Powder Sample	True Particle Density (g/cm^3)
Virgin	7.922 (0.005)
Reused	7.893 (0.005)

Single crystal δ ferrite particles form with reuse

Sandia National Laboratories

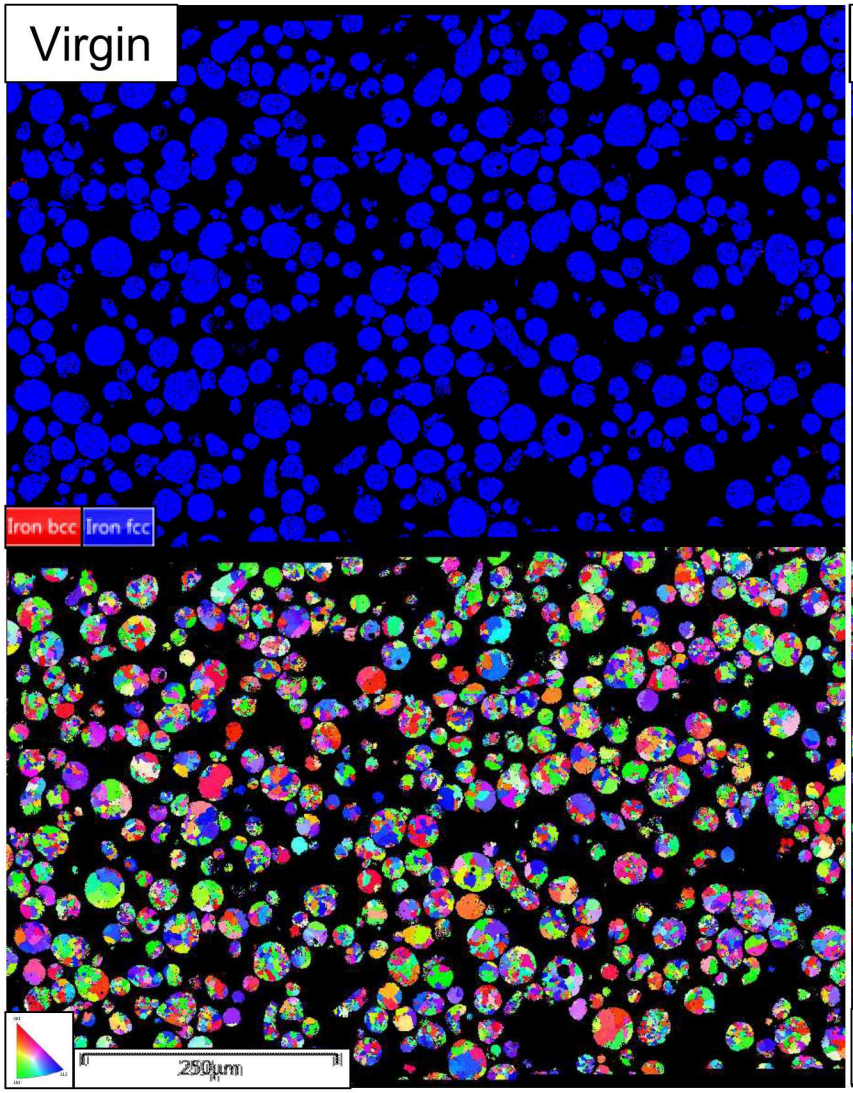

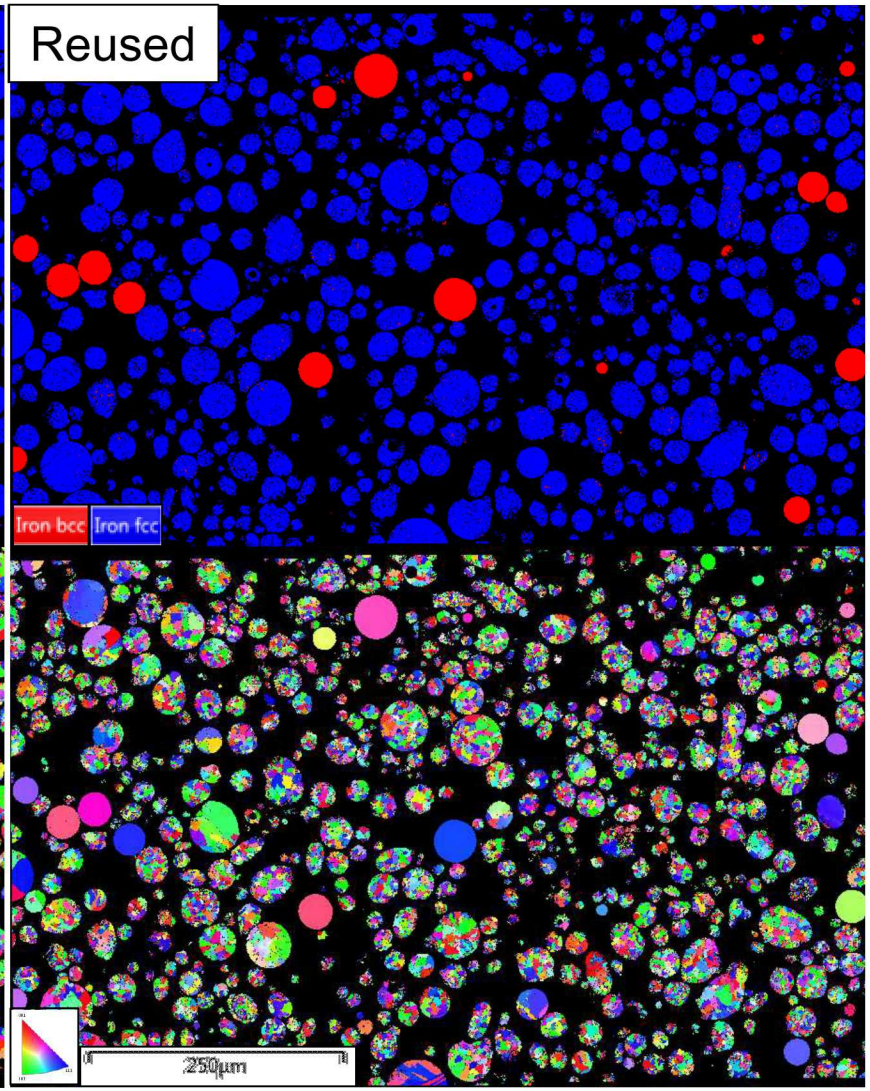

Powder (Stdev)	Grain Size (µm)	Min (µm)	Max (µm)	Iron BCC (%)	Iron FCC (%)
Virgin	4.0 (2.8)	1.8	32.3	0.30	99.70
Reused	3.3 (2.1)	1.8	46.5	6.79	93.21

- Generally austenitic in nature
- Where do these particles come from?

No major composition changes between polycrystalline and single crystal particles

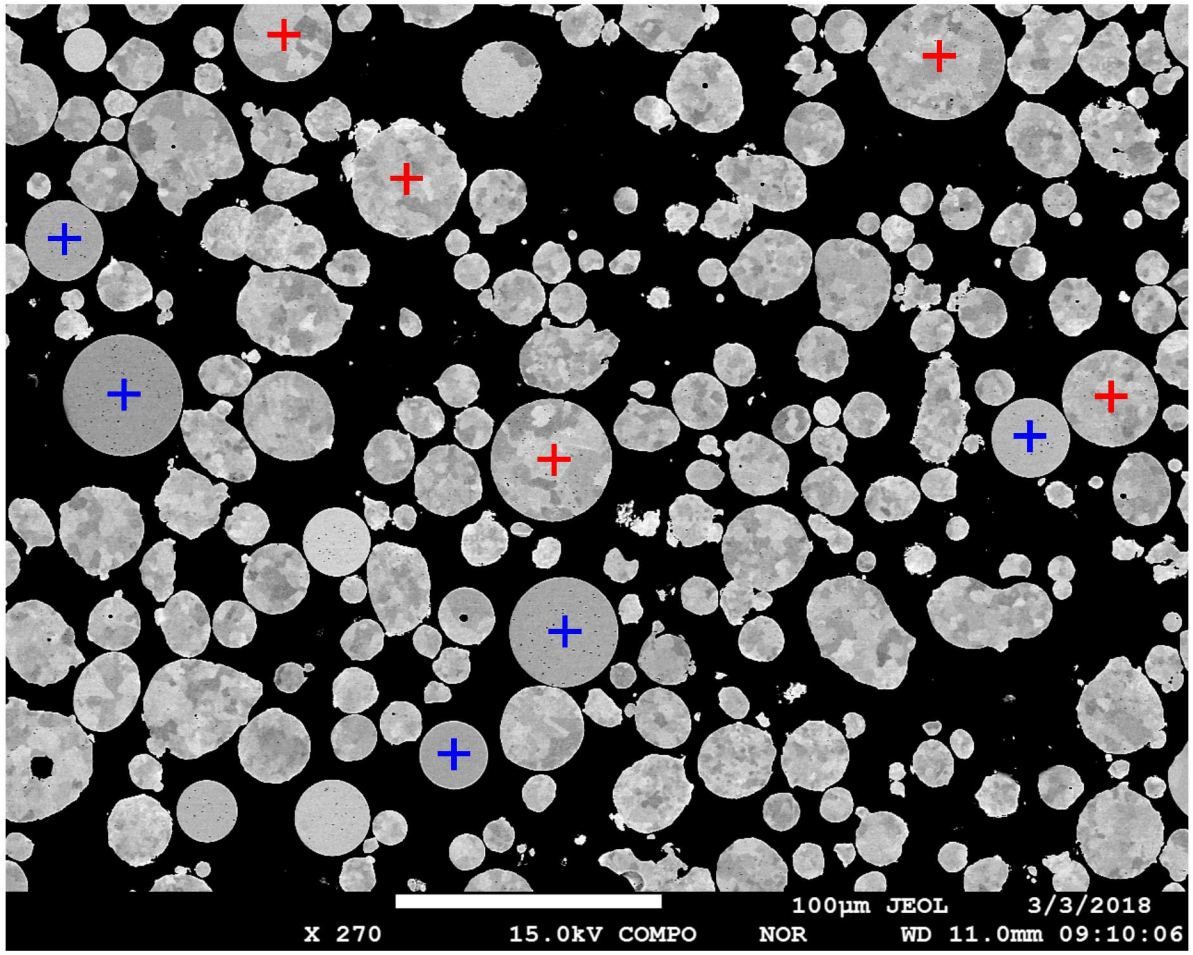

Average wt. %	Si	Mo	Mn	Ni	Cr	Fe
Virgin particle	0.65	2.05	1.20	10.81	16.84	67.80
Single Grain +	0.50	2.16	1.00	10.46	17.52	68.36
Polycrystalline +	0.58	1.98	1.28	10.65	17.49	68.03

- WDS microprobe showed that reused particles had slightly more Cr and lower Ni content than virgin state
- Cr/Ni equivalencies doesn't deviate much between polycrystalline and single crystal states
- Suggests single crystal formation is not compositionally driven

Single crystals are the result of spatter generated from both AM melt pool and gas entrainment

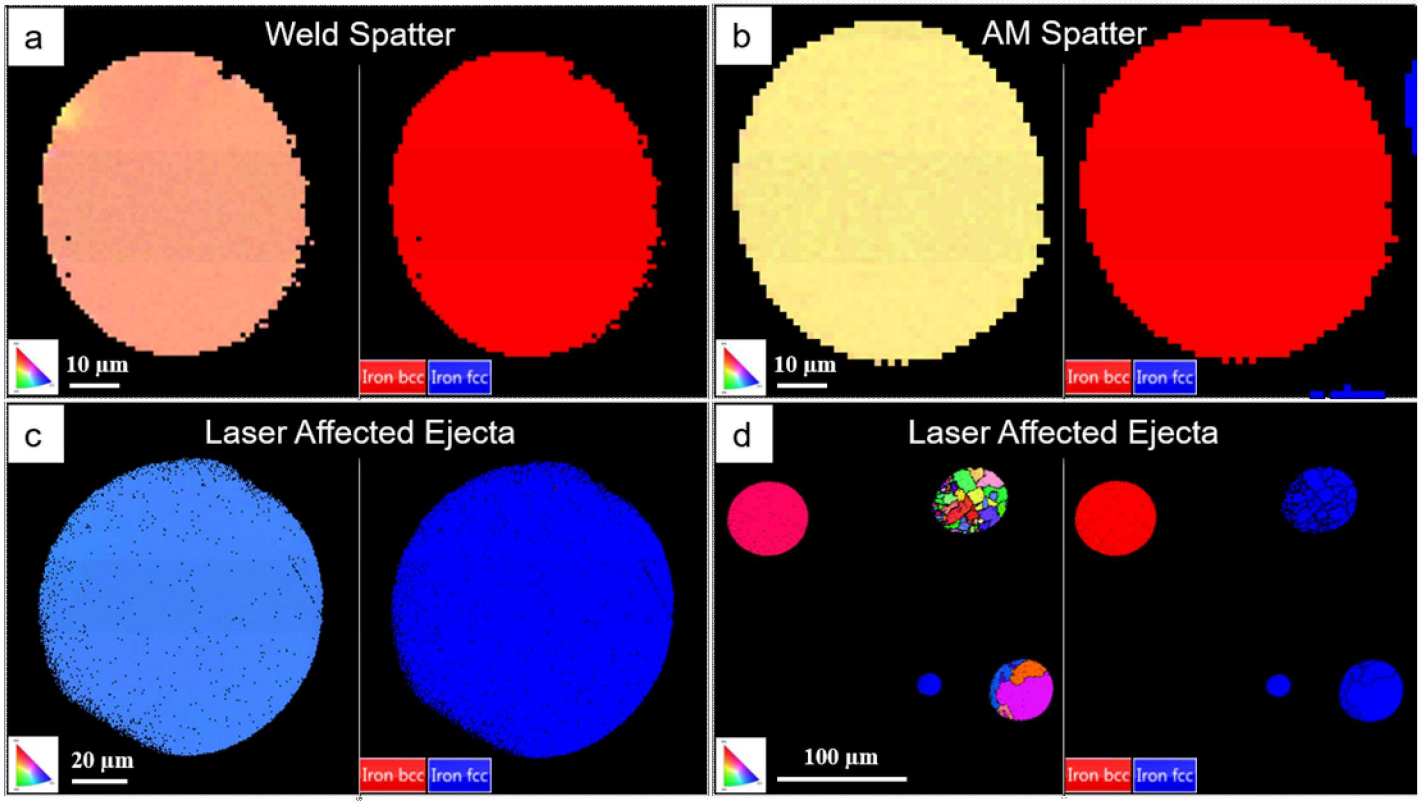

- (a) Separate weld pool experiment from two adjoining plates used to simulate melt pool particle generation – results in single crystal ferrite like (b) AM spatter
- (c & d) Pulsed laser was passed over loose powder particles to investigate changes to morphology during gas entrainment – results in same results, including single crystal austenite

Single crystal formation due to massive solidification and supercooling

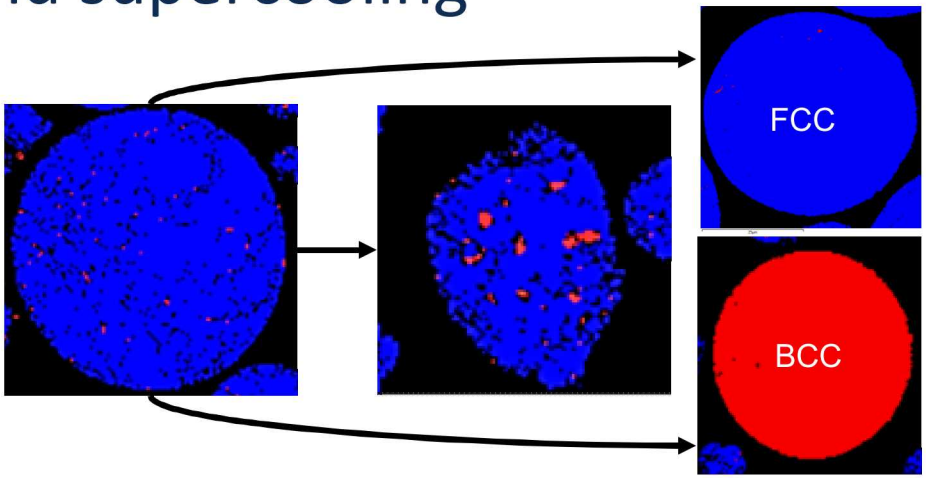

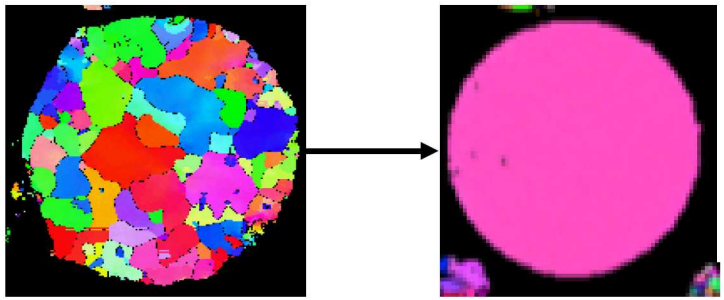

- Austenite is the primary crystallization phase of 316L stainless steel
- Kelly et al. and Cohen et al. show resulting solidification structure is a function of undercooling before nucleation, nucleation density, and particle size
- For smaller metal droplets (< 70 μm) that undergo massive solidification through supercooling (>10^5 K/s), noncellular, single crystal BCC can form

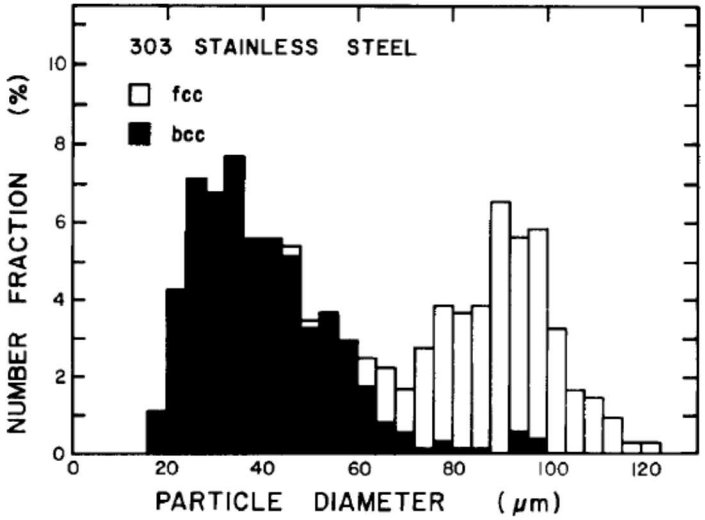

Fig. 2—Size distribution histogram of rapidly solidified 303 stainless steel powder according to crystal structure.

T. Kelly, M. Cohen, J. Vander Sande, "Rapid Solidification of a droplet-processed stainless steel, Met Trans A, 15A (1984) 819-833

T. Kelly, J. Vander Sande, M. Cohen, "FCC and BCC Solidification Products in a Rapidly Solidified Austenitic Steel", Proceedings of Materials Research Society Symposium, (1981)
M. Cohen, B. Kear, R. Mehrabian, "Rapid Solidification Processing, An Outlook", Proceedings of the 2nd Conference on Rapid Solidification Processing-Principles and Technologies, (1980)

Single crystal formation due to massive solidification and supercooling

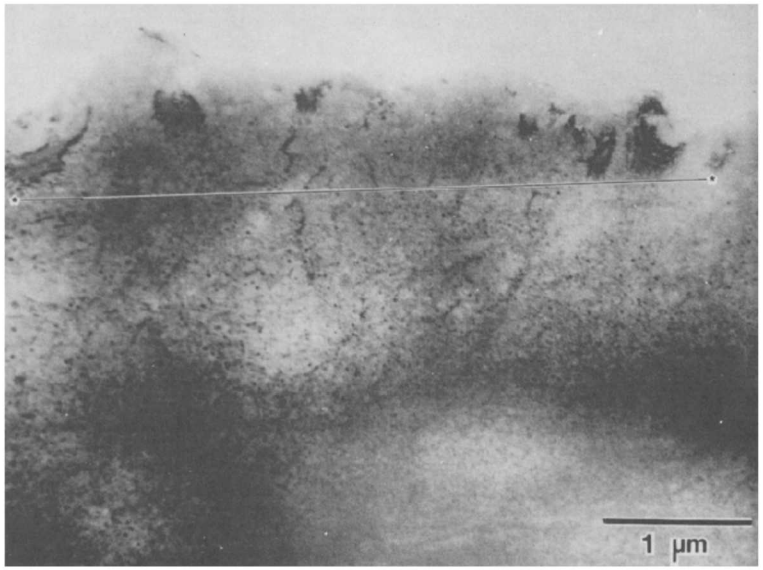

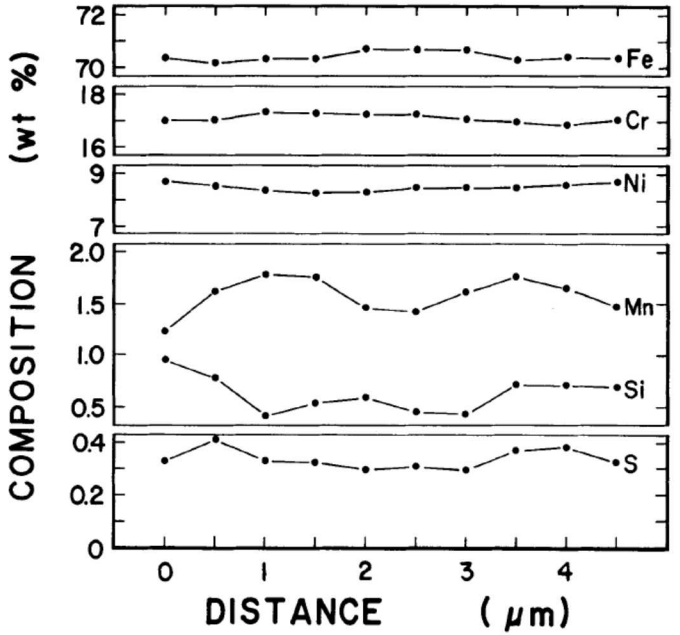

Fig. 7—Rapidly solidified noncellular bcc 303 stainless steel. Scanning transmission electron microscope bright-field image and compositional profile.

- Composition of elements is fairly constant throughout BCC particle (Kelly et al.)
- Cooling rate required to achieve massive solidification becomes less drastic with decreasing number and potency of the heterogeneous nucleation sites.
- For greater liquid supercoolings, it is possible that FCC can solidify massively, but the reason for this is not clearly understood

T. Kelly, M. Cohen, J. Vander Sande, "Rapid Solidification of a droplet-processed stainless steel, Met Trans A, 15A (1984) 819-833

Limited change to part mechanical properties with reuse

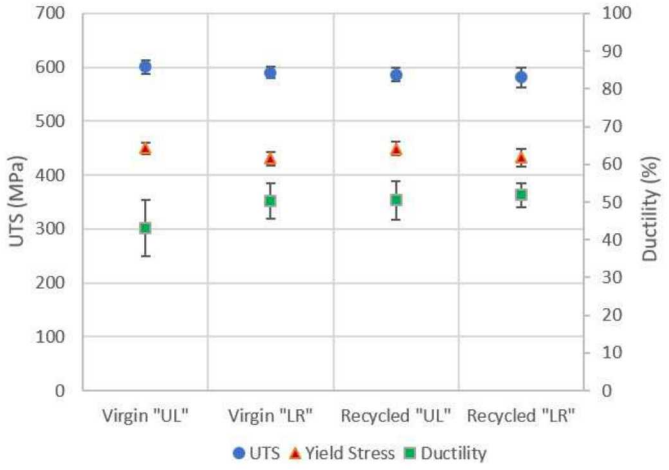

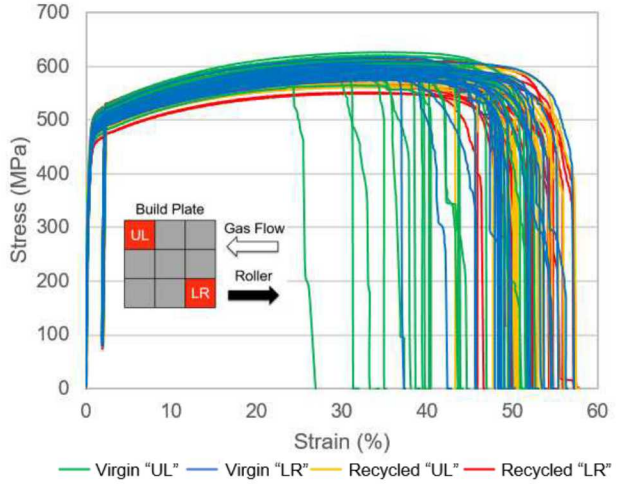

Powder Sample (Stdev)	UTS (MPa)	Yield Stress (MPa)	Elongation (%)
Virgin (UL)	600 (13)	450 (10)	43 (7)
Virgin (LR)	590 (11)	430 (13)	50 (5)
Reused (UL)	587 (12)	449 (12)	50 (5)
Reused (LR)	582 (19)	433 (17)	52 (3)

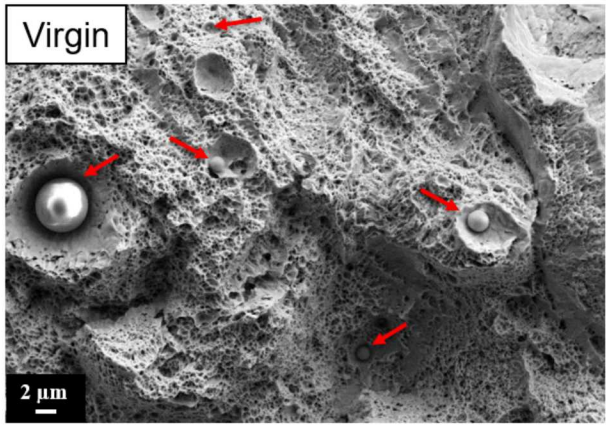

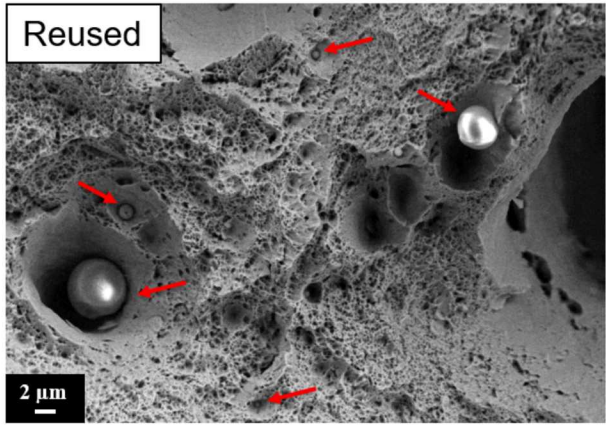

Virgin: 7.90 g/cm^3 (98.72% density)

Reused: 7.81 g/cm^3 (97.65% density)

- Location on build plate appears to play more of a role in affecting properties than reuse state for 316L
- However, virgin powder-built parts tend to have more variable ductility

No major changes to part microstructure with reuse

Virgin - Longitudinal

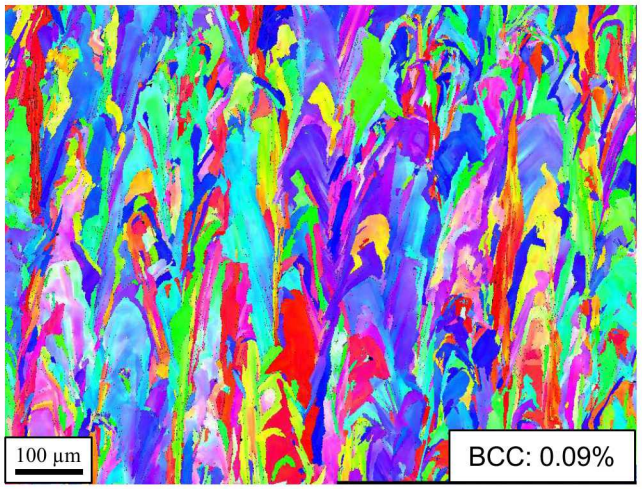

Virgin - Transverse

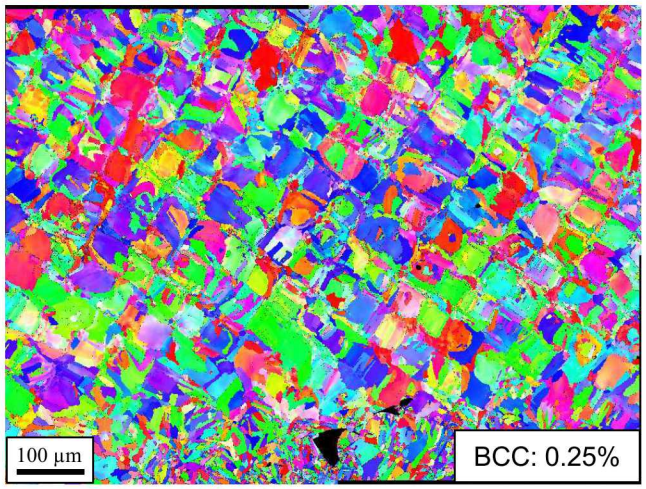

Virgin – Longitudinal Z

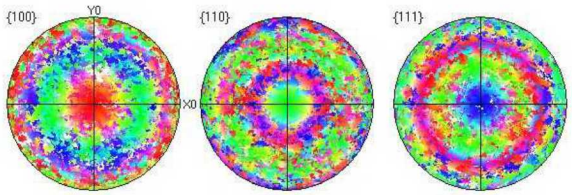

Virgin – Transverse

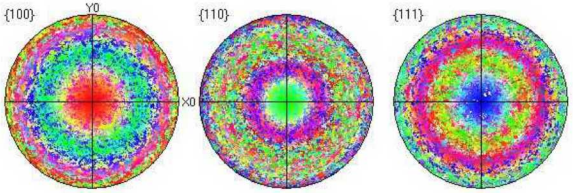

Reused - Longitudinal

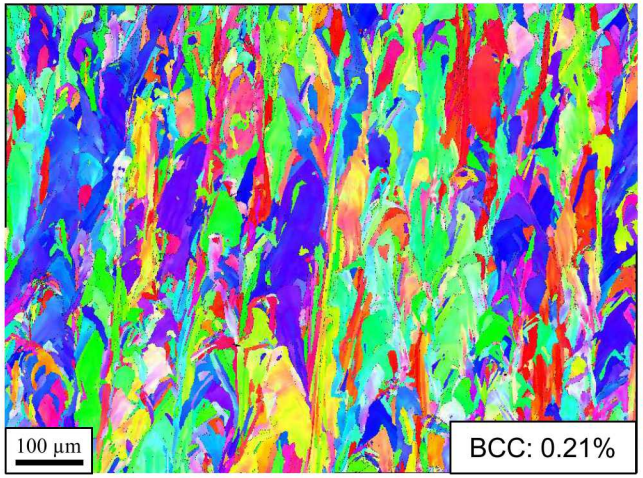

Reused - Transverse

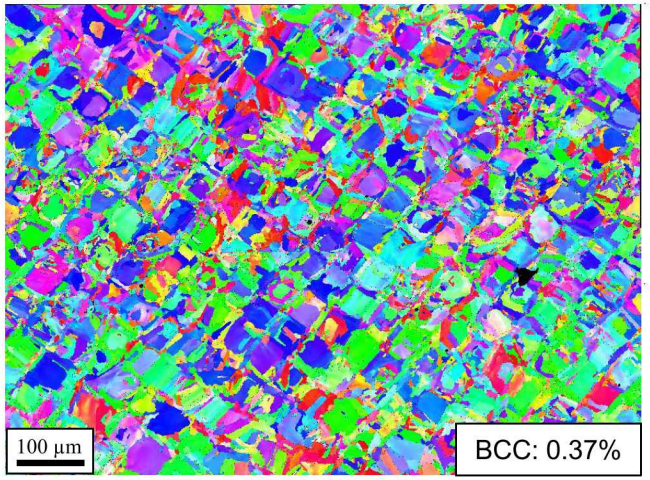

Reused – Longitudinal

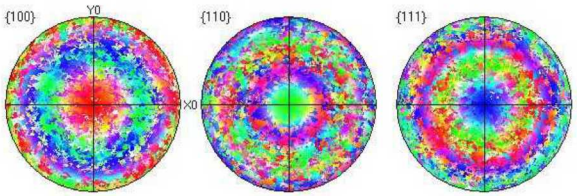

Reused – Transverse

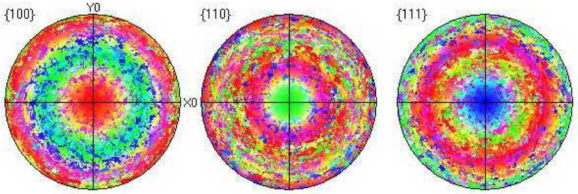

- There were no significant changes between virgin and reused part microstructures.

Significant increase in C and O in built parts with 30x reuses

Sandia National Laboratories

Built Parts

Wt.% (Stdev)	Fe	Cr	Ni	Mo	Si	Mn	Cu	P	Co	C	S	O	N
Virgin	67.7 (0.3)	16.70 (0.33)	10.75 (0.26)	2.07 (0.21)	0.62 (0.09)	1.11 (0.11)	0.24 (0.04)	0.020 (0.003)	0.11 (0.02)	0.14 (0.02)	0.014 (0.002)	0.21 (0.03)	0.080 (0.012)
Reused	67.8 (0.3)	16.77 (0.33)	10.68 (0.21)	2.02 (0.20)	0.55 (0.08)	1.25 (0.12)	0.25 (0.04)	0.022 (0.003)	0.13 (0.02)	0.19 (0.03)	0.011 (0.002)	0.14 (0.02)	0.090 (0.013)

Initial Powder

Virgin	67.8 (0.3)	16.84 (0.34)	10.81 (0.22)	2.05 (0.20)	0.65 (0.10)	1.20 (0.12)	0.21 (0.03)	0.015 (0.002)	0.098 (0.015)	0.011 (0.002)	0.014 (0.002)	0.067 (0.010)	0.086 (0.013)
Reused	67.6 (0.3)	16.91 (0.34)	10.90 (0.22)	2.02 (0.20)	0.60 (0.09)	1.27 (0.13)	0.22 (0.03)	0.016 (0.002)	0.11 (0.016)	0.016 (0.002)	0.014 (0.002)	0.095 (0.014)	0.090 (0.013)
ASTM Spec [2]	61-69	16-18	10-14	2-3	1 max	2 max	-	0.045 max	-	0.03 max	0.03 max	-	-

- Carbon and Oxygen both increased with reuse in powder. However, only Carbon increased with reuse in the actual parts. Oxygen content decreased.
- Carbon content is actually out of ASTM spec on the part themselves

[2] ASTM F3184-16 Standard Specification for Additive Manufacturing Stainless Steel Alloy (UNS S31603) with Powder Bed Fusion, ASTM International ASM Handbook (2016) 1-9.

Despite significant changes to powder properties with reuse, 316L powder is fairly robust

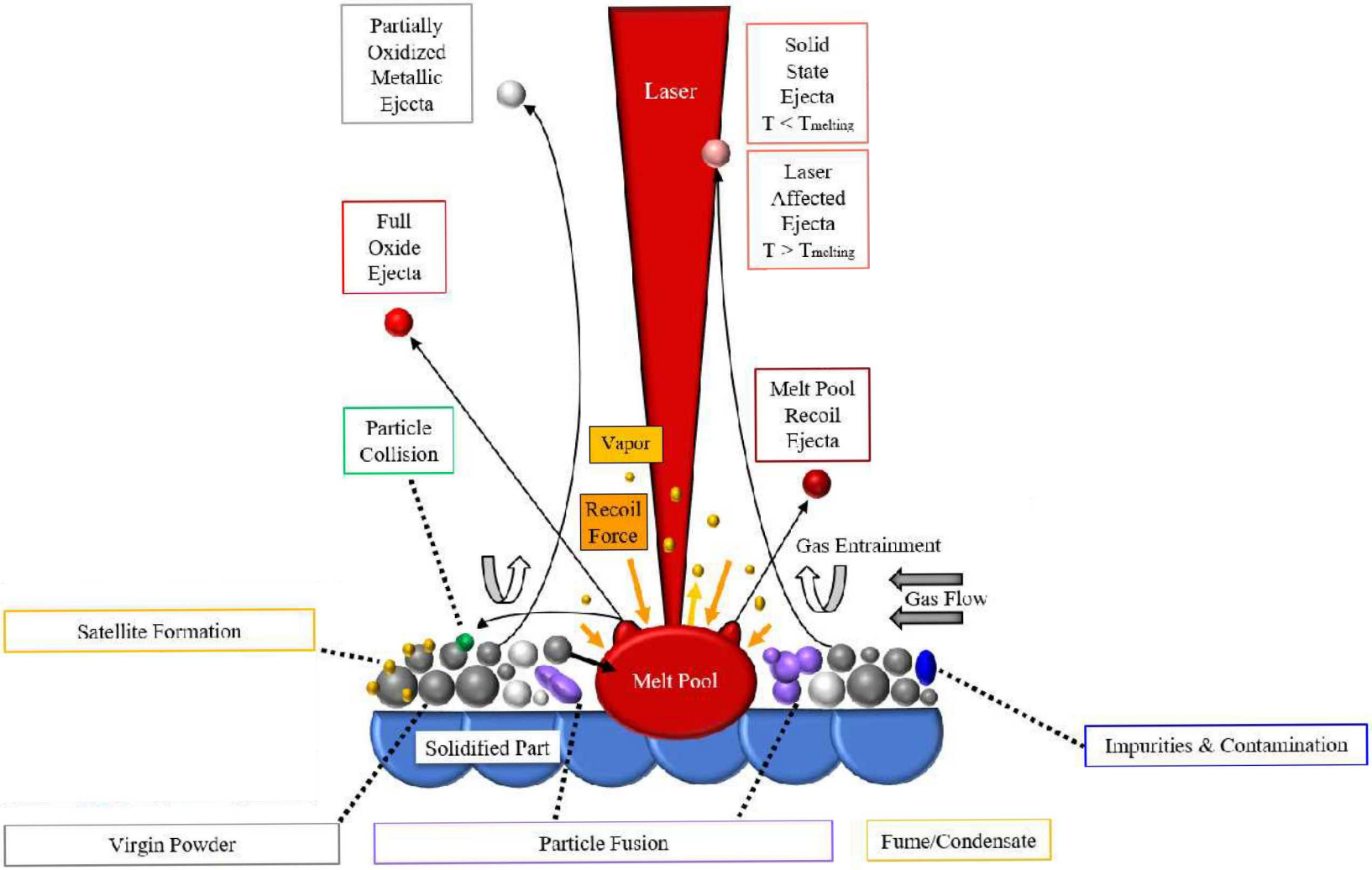

Acknowledgements

- Ana Baca
- Mike Brumbach
- Rebecca Chow
- Jeff Reich
- Mark Rodriguez
- Christina Profazi
- Ping Lu
- Lisa Lowery
- Tod Monson
- Charles Pearce
- Sara Dickens
- Harlan Brown-Shacklee
- James Griego
- Chris DiAntonio
- Julie Gibson
- Thomas Diebold
- Jay Carroll
- Dick Grant
- Alexander Barr
- Matthew Vieira
- Richard Grant
- Joe Michael
- Todd Huber

Paper: (Under Review)

M. Heiden, L. Deibler, J. Rodelas, J. Koepke, D. Tung, D. Saiz, B. Jared, Evolution of 316L Stainless Steel Feedstock Due to Laser Powder Bed Fusion Process. Additive Manufacturing.

Sandia National Laboratories is a multi-mission laboratory managed and operated by National Technology and Engineering Solutions of Sandia, LLC., a wholly owned subsidiary of Honeywell International, Inc., for the U.S. Department of Energy's National Nuclear Security Administration under contract DE-NA-0003525. Internal Presentation 2018

Appendix: Characterization Methods

Sandia National Laboratories

Property Measured	Metrology Methods Employed
Particle size distribution	Cross section/optical microscopy, scanning electron microscopy (SEM), x-ray micro-computed tomography (μCT), laser diffraction
Aspect ratio	Cross section/optical microscopy, SEM, μCT
Circularity	Cross section/optical microscopy, SEM, μCT
Internal porosity	Cross section/microscopy, SEM, μCT
True particle density	Helium pycnometry
Grain size	Cross section/etching, SEM/EBSD, transmission electron microscopy (TEM)
Crystal structure/phase	X-ray diffraction (XRD), SEM/EBSD, TEM
Oxide thickness	TEM
Hardness	Nanoindentation
Magnetic susceptibility/coercivity	Vibrating sample magnetometer (VSM)
Bulk composition	Inductively coupled plasma mass spectrometry (ICP-MS), SEM/EDS, electron microprobe analyzer (EMPA)
Surface composition	Auger spectroscopy, x-ray photoelectron spectroscopy (XPS)
Surface Roughness	Atomic force microscopy (AFM), confocal laser scanning microscopy

Surface Finish – AFM and Confocal

AFM analysis area: 5 μm^2

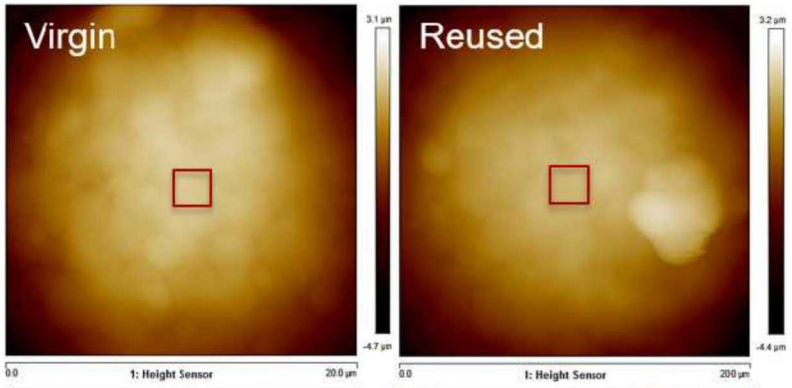

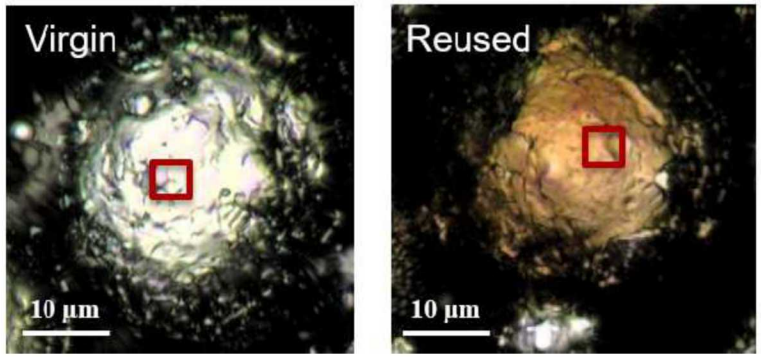

Confocal Microscope analysis area: 20 μm^2

- Curvature corrections applied to both techniques
- Larger “macroscale” roughness with reuse; higher amount of satellites
- Virgin particles have higher “underlying” roughness, due to dendritic grooves
- Reused particles have better surface finish; may be from deformation or heat treatment during laser process

Average Surface Roughness S_a (Stdev)	Confocal Microscopy (Including Satellites) (nm)	AFM (Between Satellites) (nm)
Virgin	127 (53)	23 (9)
Reused	135 (66)	10 (7)

X-ray Diffraction

Sandia National Laboratories

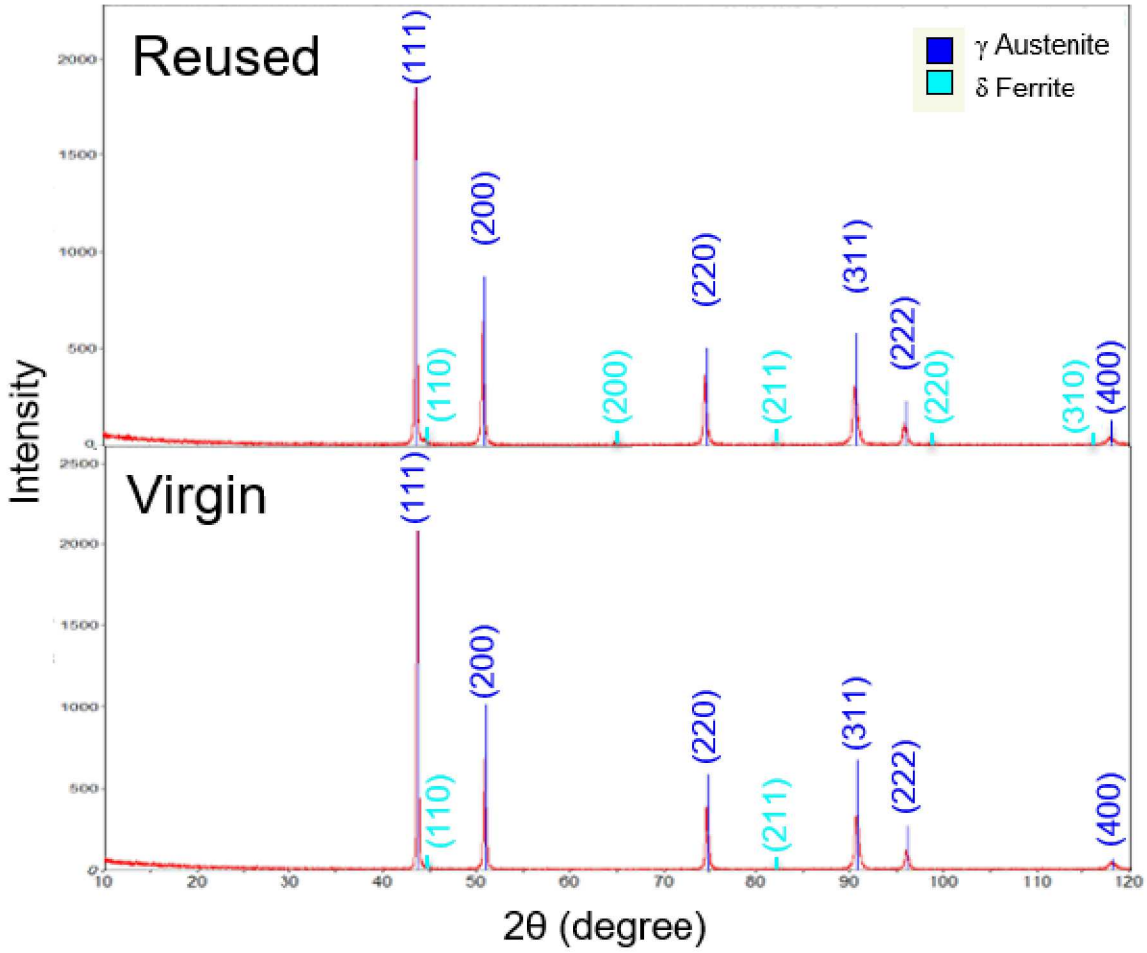

- Virgin: γ (FCC) austenite phase, with 0.5% δ (BCC) ferrite phase
- Reused: γ (FCC) austenite phase, with 1.6% δ (BCC) ferrite phase

Surface Composition - XPS

Wt. % (Stdev)	O	C	Fe	Si	Mn	Cr	N	S
Virgin	33.1 (0.4)	15.3 (0.8)	25.4 (2.0)	9.3 (0.4)	9.3 (0.5)	6.7 (0.2)	0.4 (0.3)	0.4 (0.1)
Reused	30.4 (0.1)	17.6 (0.4)	29.1 (1.2)	6.4 (0.4)	11.5 (0.5)	3.9 (0.0)	0.4 (0.0)	0.7 (0.1)

- Metallic component peaks for Fe (708-708 eV) and Cr (574-575 eV) reduced with reuse
- Suggests thicker oxide

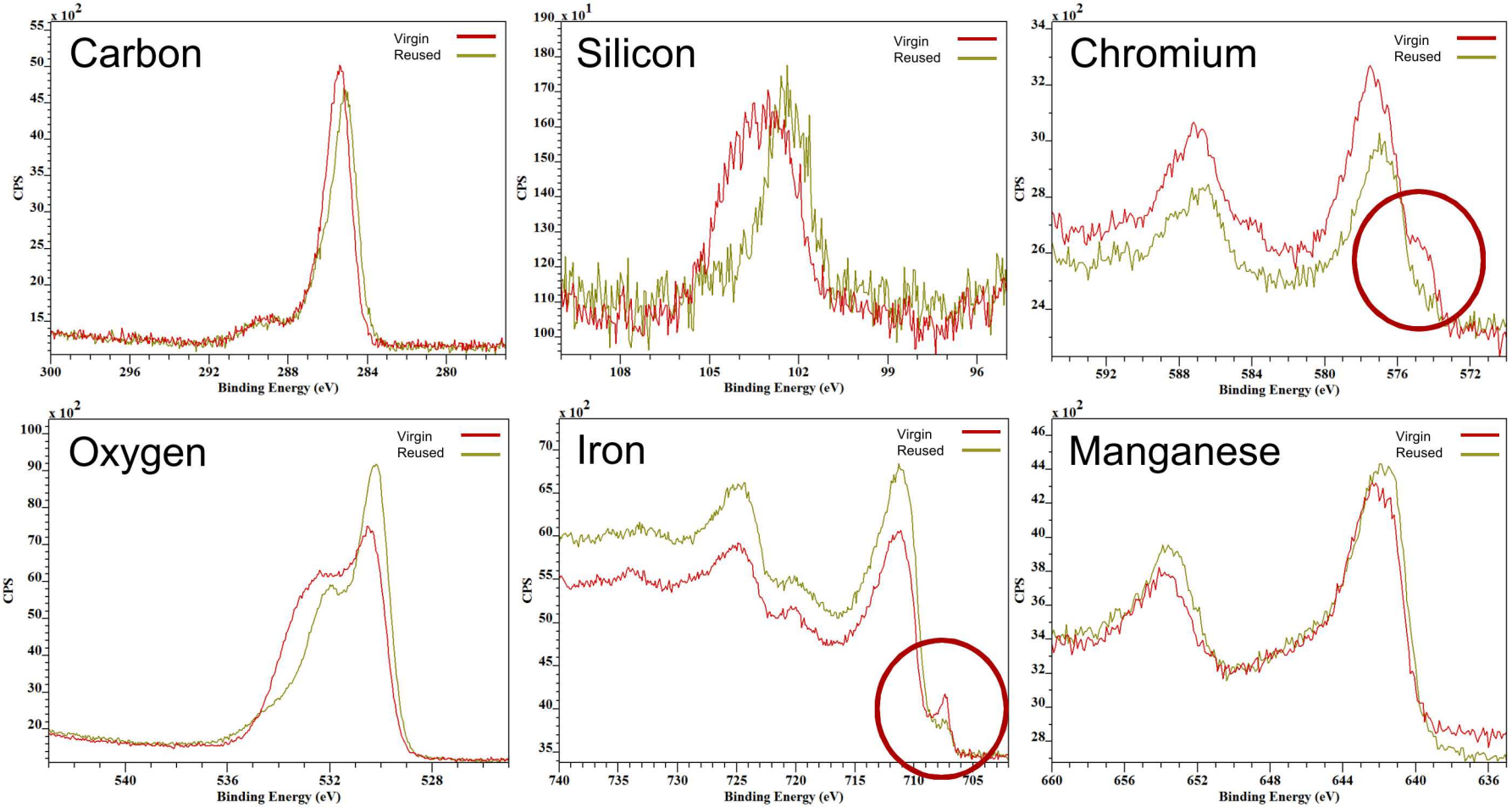

Particle Size Comparisons

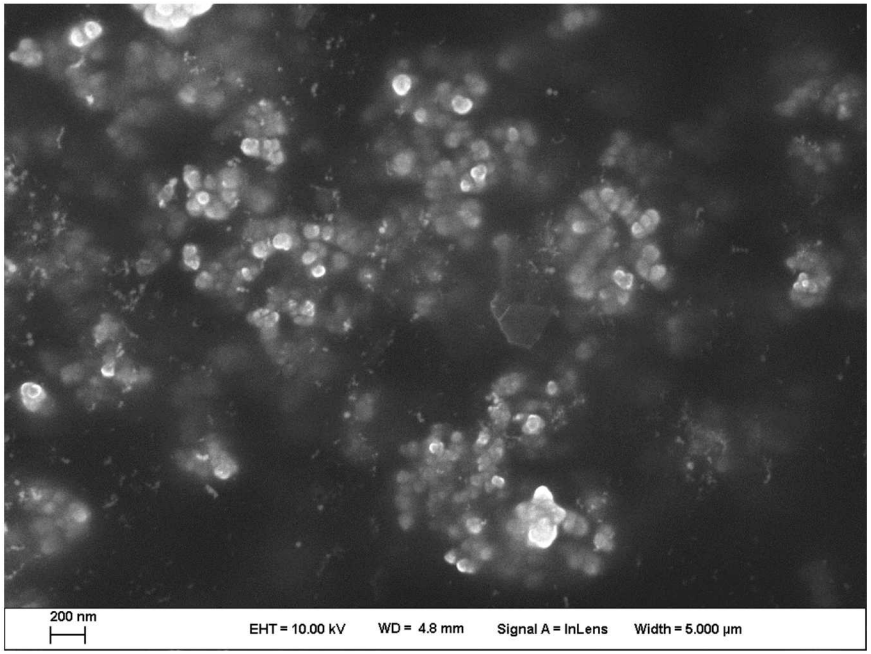

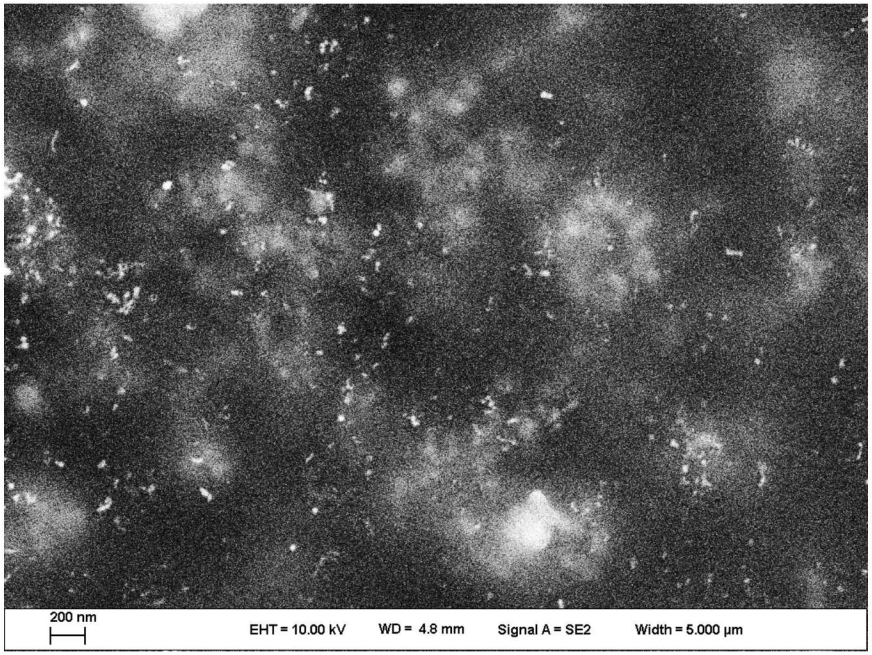

Powder (Stdev)	Larger Fume (nm)	Ultrafine Fume (nm)	Wall Spatter (µm)	Sieved (µm)	AM Spatter (µm)	Weld Spatter (µm)
Average Diameter	77.8 (18.7)	29.8 (9.0)	20.9 (9.3)	33.6 (18.1)	33.5 (14.6)	124.3 (45.3)
Max	138.0	49.8	54.1	101.6	72.5	226.5
Min	47.9	12.4	4.2	5.6	4.0	52.7

- Fume is hierarchical in nature
- One source of satellite formation and laser muting of machine lens

Oxide Thickness - TEM

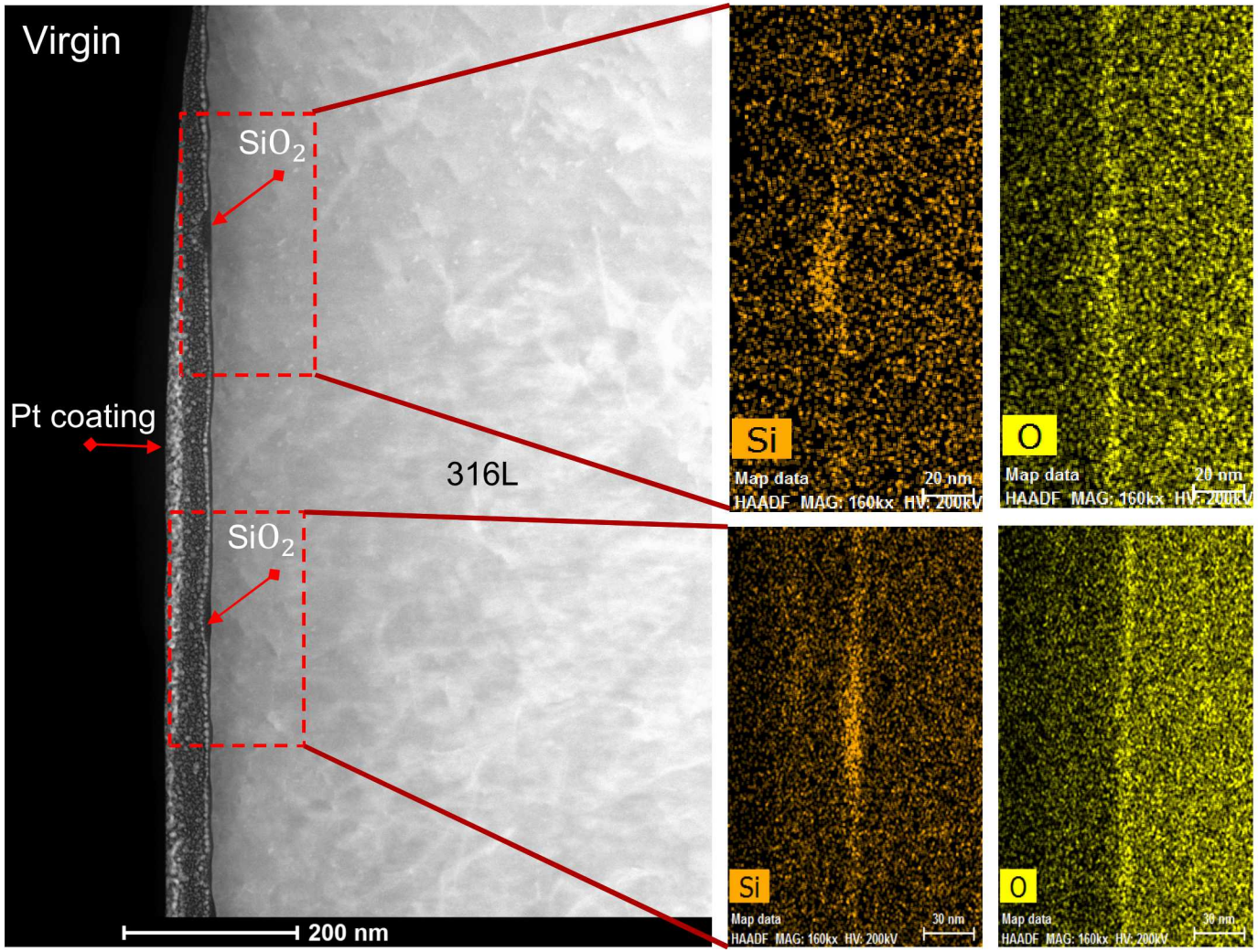

- Virgin oxide layer is composed of SiO_2
- Average oxide thickness is ~3-4 nm
- Thicker ~15 nm nodules tend to form near the end of grain boundaries

Oxide Thickness - TEM

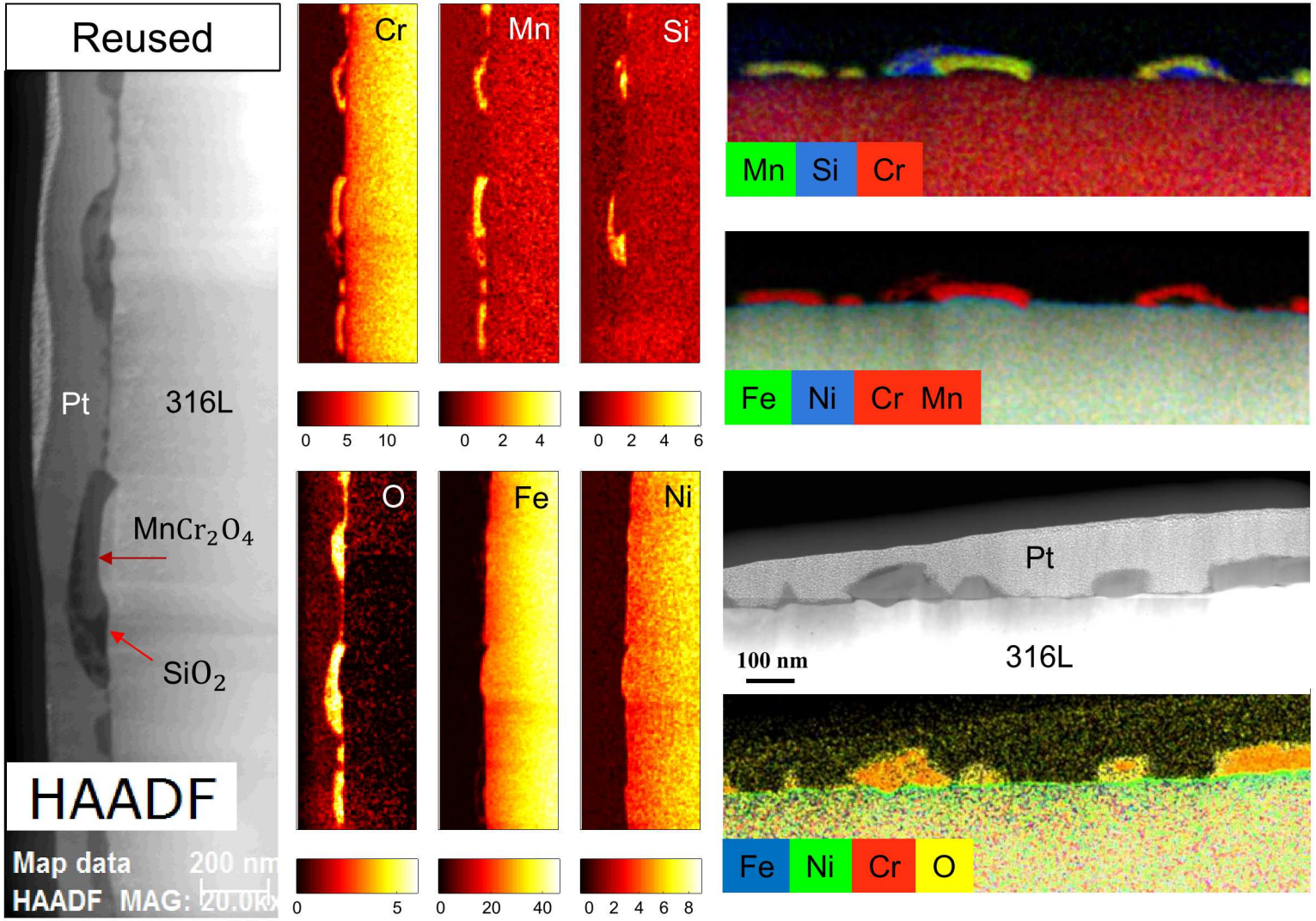

- Reused particles form $MnCr_2O_4$ and larger SiO_2 nodules across the surface
- Mn and Cr depleted zone beneath the oxide layer

Surface Composition - Auger

Irregular, characteristically rough particles								
Wt. % (Stdev)	O	C	Fe	Si	Mn	Cr	Ni	S
Virgin	23.2 (5.1)	9.7 (1.0)	41.9 (5.5)	6.0 (2.3)	-	15.8 (9.1)	3.0 (1.7)	0.4 (0.2)
Reused	34.2 (3.0)	12.2 (4.4)	38.2 (3.7)	9.9 (2.6)	-	-	4.7 (2.4)	0.8 (0.1)
Round, characteristically smooth particles								
Wt. % (Stdev)	O	C	Fe	Si	Mn	Cr	Ni	S
Virgin	30.5 (2.8)	6.2 (1.0)	52.8 (7.0)	10.5 (5.9)	-	-	-	-
Reused	22.4 (3.7)	5.9 (2.7)	28.5 (2.0)	18.7 (1.5)	24.5 (1.4)	-	-	-

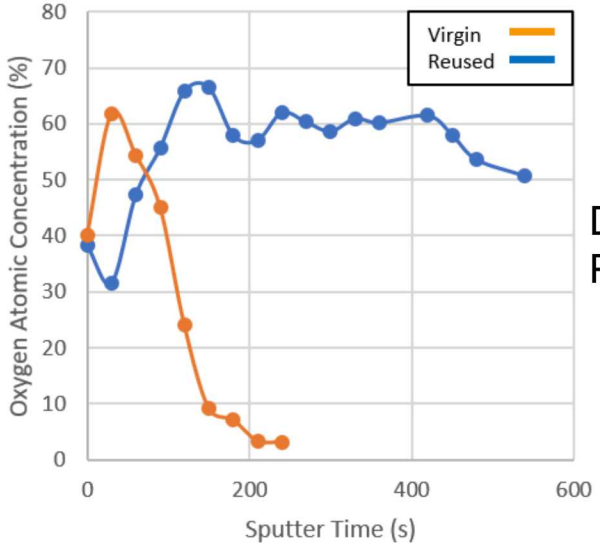

Depth Profiling

- C, Si, Mn increased for smooth
- O, Si, Ni, S increased for rough
- Depth profiling showed increase in oxide thickness with reuse

Round

Irregular

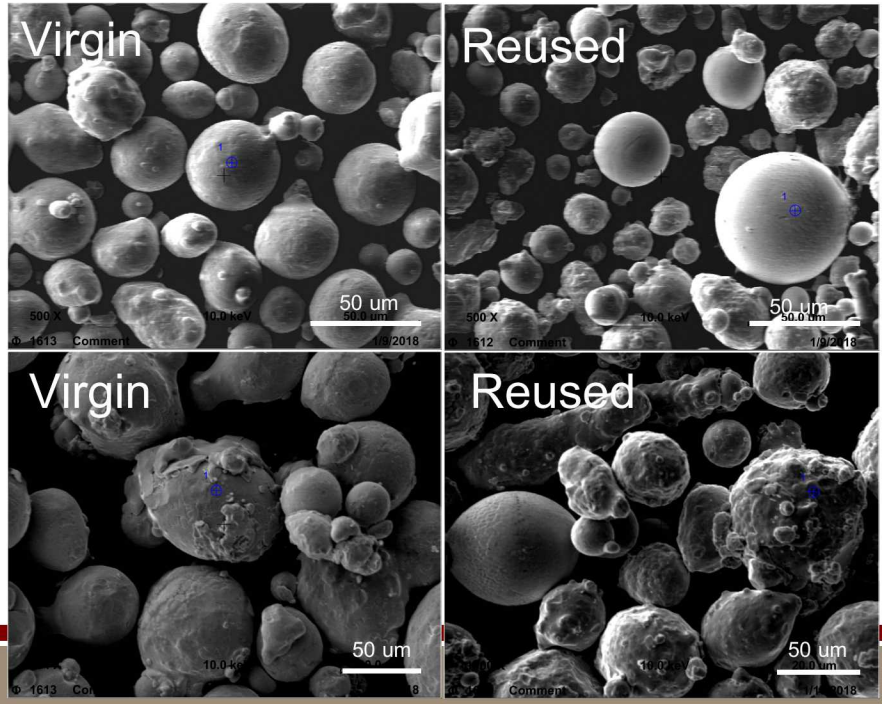

Micro CT scans

Virgin

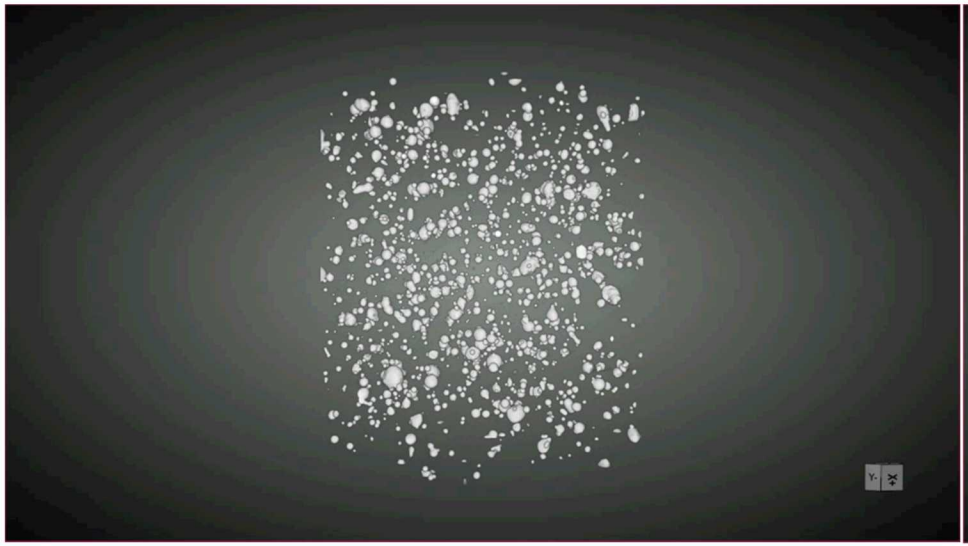

Reused

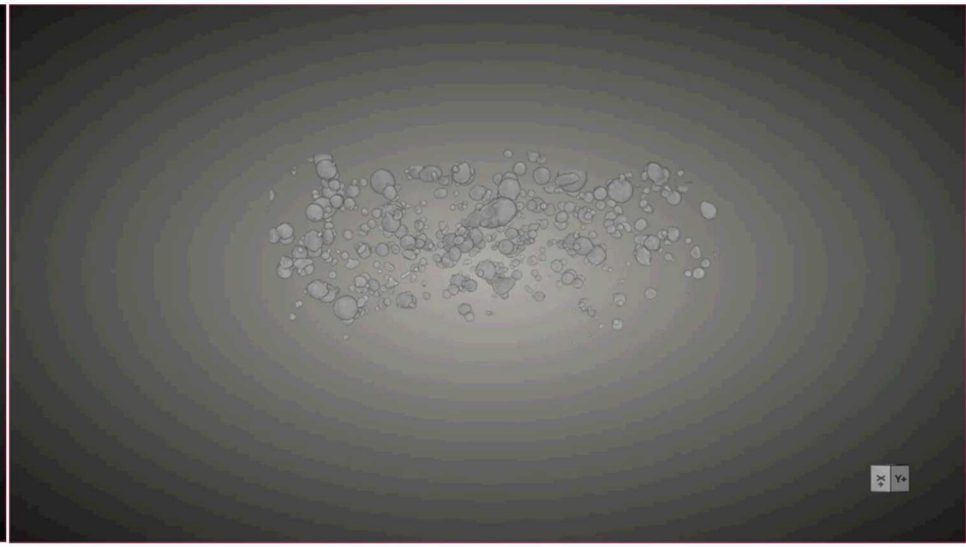

Powder (Stdev)	Average Diameter (μm)	Average Aspect Ratio
Virgin	15.5 (6.5)	0.75 (0.18)
Reused	18.54 (8.4)	0.68 (0.20)
Sieved	39.1 (26.0)	0.61 (0.19)
Virgin Pores	7.0 (2.4)	0.91 (0.03)
Reused Pores	4.4 (1.6)	0.77 (0.11)

- Fines reduced greatly
- Average diameter increases with reuse
- Reused pore size slightly smaller
- Aspect ratio slightly reduced with reuse

Magnetic Susceptibility

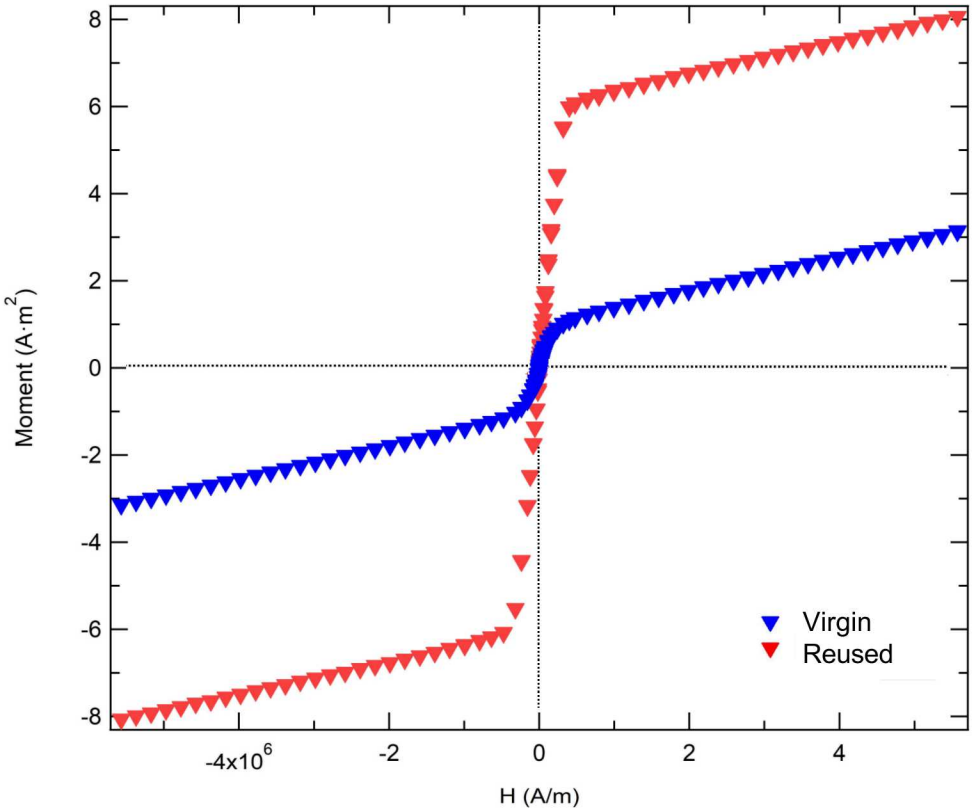

Powder Sample	Moment at 7T (Am^2/kg)	Coercivity (A/m)	Susceptibility
Virgin	3.137	4651.53	7.07E-06 (2.89E-07)
Reused	8.065	1383.80	2.38E-05 (3.84E-07)

- Significant increase in magnetic susceptibility of reused powder
- Reused powder has a higher max magnetic moment (strength of magnetization)
- Virgin power has a higher coercivity; harder to demagnetize

$$\chi_m = \frac{M}{H}$$

Weld Spatter Oxide

AM Spatter Oxide

EDS Weld Spatter

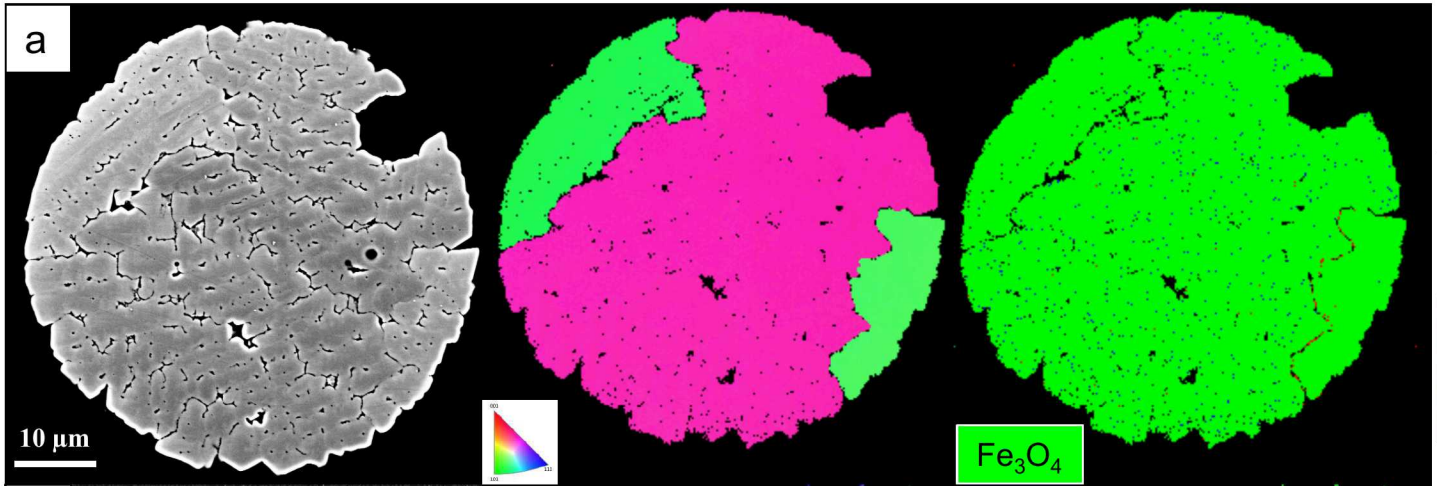

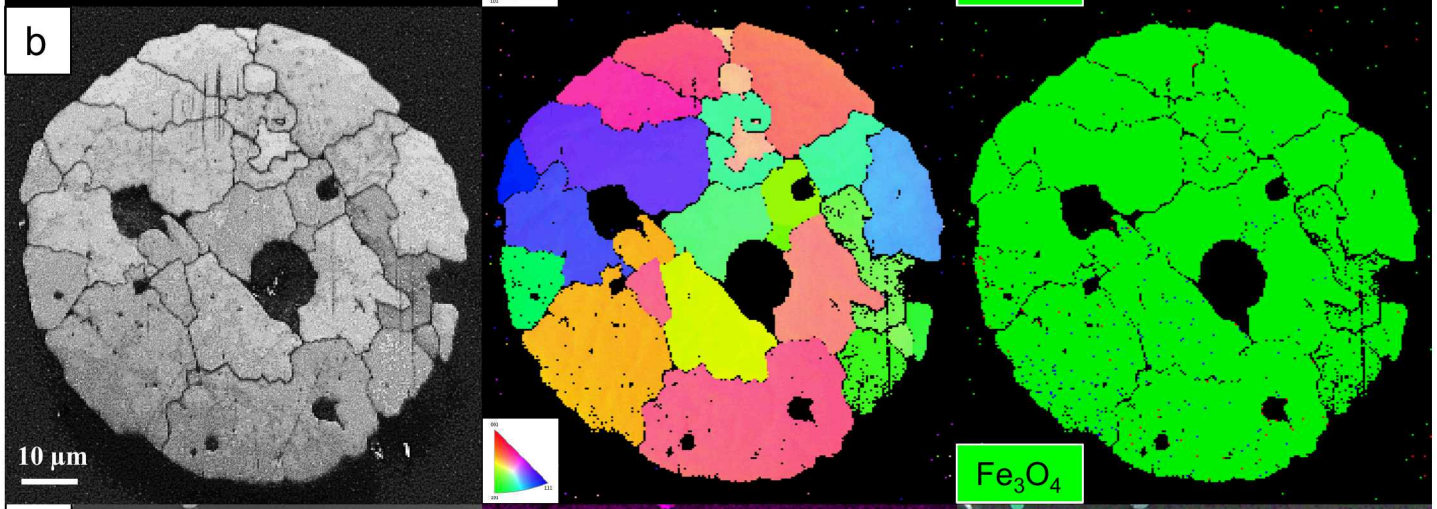

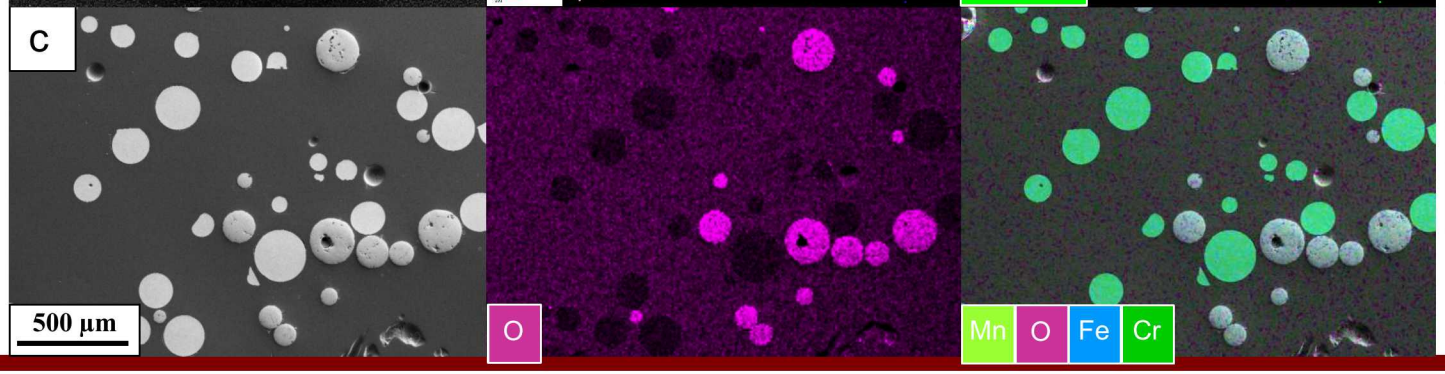

Sandia National Laboratories

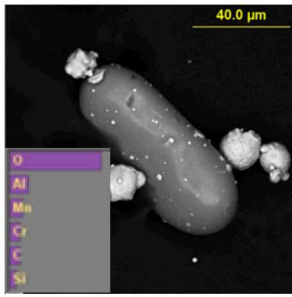

Oxide

Fe_3O_4: 98.84%
Fcc: 0.96%
Bcc: 0.20%

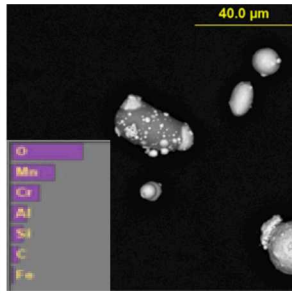

Oxide